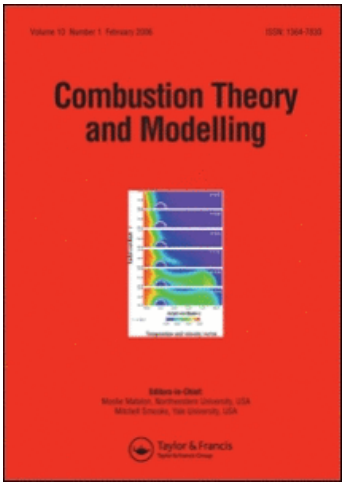

Combustion Theory and Modelling
Publication details, including instructions for authors and subscription information:
http://www.informaworld.com/smpp/title~content=t713665226

Flame balls with thermally sensitive intermediate kinetics

J. W. Dold[a]; R. O. Weber[b]; R. W. Thatcher[a]; A. A. Shah[c]
[a] Mathematics Department, UMIST, Manchester, UK [b] School of Mathematics and Statistics, UNSW at ADFA, Canberra, Australia [c] Fuel and Energy Department, University of Leeds, Leeds, UK

Online publication date: 28 February 2002

To cite this Article Dold, J. W. , Weber, R. O. , Thatcher, R. W. and Shah, A. A.(2003) 'Flame balls with thermally sensitive intermediate kinetics', Combustion Theory and Modelling, 7: 1, 175 — 203
To link to this Article: DOI: 10.1088/1364-7830/7/1/310
URL: http://dx.doi.org/10.1088/1364-7830/7/1/310

INSTITUTE OF PHYSICS PUBLISHING COMBUSTION THEORY AND MODELLING

Combust. Theory Modelling **7** (2003) 175–203 PII: S1364-7830(03)33511-9

Flame balls with thermally sensitive intermediate kinetics

J W Dold[1], R O Weber[2], R W Thatcher[1] and A A Shah[3]

[1] Mathematics Department, UMIST, Manchester M60 1QD, UK
[2] School of Mathematics and Statistics, UNSW at ADFA, Canberra, Australia
[3] Fuel and Energy Department, University of Leeds, Leeds LS2 9JT, UK

E-mail: John.Dold@umist.ac.uk

Received 6 February 2002, in final form 11 October 2002
Published 28 February 2003
Online at stacks.iop.org/CTM/7/175

Abstract

Spherical flame balls are studied using a model for the chemical kinetics which involves a non-exothermic autocatalytic reaction, describing the chain-branching generation of a chemical radical and an exothermic completion reaction, the rate of which does not depend on temperature. When the chain-branching reaction has a large activation temperature, an asymptotic structure emerges in which the branching reaction generates radicals and consumes fuel at a thin flame interface, although heat is produced and radicals are consumed on a more distributed scale. Another model, based more simply, but less realistically, on the generation of radicals by decomposition of the fuel, provides exactly the same leading order matching conditions. These can be expressed in terms of jump conditions across a reaction sheet that are linear in the dependent variables and their normal gradients. Using these jump conditions, a reactive–diffusive model with linear heat loss then leads to analytical solutions that are multivalued for small enough levels of heat loss, having either a larger or a smaller radius of the interface where fuel is consumed. The same properties are found, numerically, to persist as the activation temperature of the branching reaction is reduced to values that seem to be typical for hydrocarbon chemistry. Part of the solution branch with larger radius is shown to become stable for low enough values of the Lewis number of the fuel.

1. Introduction

A paradigm in combustion theory, that has dominated the modelling and study of flames from a theoretical and analytical perspective, is the use of a one-step model to describe the chemistry [1–13], such as

$$\mathrm{F} + \mathrm{M} \rightarrow \mathrm{P} + \mathrm{M} + \textit{heat} \qquad \text{or} \qquad \mathrm{F} + \mathrm{O}_2 \rightarrow 2\mathrm{P} + \textit{heat} \tag{1}$$

with an Arrhenius 'rate constant' $k = Ae^{-T_A/T}$. In these model reaction schemes, the fuel F is considered to produce the product P (with the intervention of an oxidant O_2 in the second example) through a single elementary chemical step. The symbol M represents any molecule that is needed to trigger the reaction step, but that is not changed by the reaction. As a result, the rate of the first reaction is taken to be proportional to $\rho^2 Y_F e^{-T_A/T}$, and the rate of the second reaction to $\rho^2 Y_F Y_{O_2} e^{-T_A/T}$, where ρ is the density and Y_F and Y_{O_2} are the mass fractions of the fuel F and the oxidant O_2, respectively.

The usefulness of this form of model lies partly in its inherent simplicity, but also partly in the fact that the asymptotic limit in which the activation temperature T_A approaches infinity proves very useful for approximating solutions analytically—the resulting extreme sensitivity of the reaction rate to changes in temperature leads to narrow regions of reaction that match with outer regions of non-reactivity, in asymptotic structures that are amenable to further study. In flames, realistic values of T_A/T are often thought to be about ten to fifteen. Moreover, the effect of changes in temperature on chemical reactivity is exaggerated by the exponential in the rate constant, so that the assumption that T_A/T is large does not seem unreasonable.

In fact, the one-step, large activation temperature asymptotic limit has led to many useful and qualitatively correct predictions for, amongst other things, such phenomena as: ignition, extinction and stability of diffusion flames; propagation and stability of premixed flames with heat loss; flame balls with heat loss and their stability at low Lewis numbers; structure and propagation of triple flames and other flame edges; and the initiation, structure and stability of detonations. With only a few exceptions (as found in [14–19]), analytical solutions describing laminar flames have been founded on the one-step model; flames have also been described using a variety of reduced-kinetic models for the chemistry [20–22], the rates of which are combinations of the rates of elementary hydrocarbon oxidation reactions, but these models are much more problematic to analyse in any general way. References for all the achievements of the one-step model are far too numerous to cite here; the reader can find many suitable citations in texts and review articles on combustion theory and in recent articles on the subject, e.g. [1–13].

Most of these results have been obtained analytically in terms of matched asymptotic descriptions in the limit as $T_A/T \to \infty$, providing an in-depth understanding of the behaviour of many experimental observations of flames. Indeed, asymptotic and numerical predictions of some phenomena, such as the negative propagation speed of the flame edges [23–26] and the existence of stable flame balls [27–33], preceded and indeed motivated their observation experimentally [26, 31–33]. There is now a growing theoretical literature of flame-ball studies based on one-step chemistry [34–42], supplemented by numerical studies based on detailed chemical, transport and radiative models [43–46].

Of course, real hydrocarbon flames do not arise as a result of one-step chemistry. There are usually very many contributing reactions involving several more chemical compounds than simply fuel, product and oxidant [47–50]. More complex models, even the relatively simple model that includes autocatalytic chain branching [1, 2, 14] of an intermediate chemical 'radical' Z

$$\begin{aligned} &\mathrm{F} + \mathrm{Z} \to 2\mathrm{Z} \quad &:& \quad k_B = A_B e^{-T_B/T} \\ &\mathrm{Z} + \mathrm{M} \to \mathrm{P} + \mathrm{M} \quad &:& \quad k_C = A_C \end{aligned} \tag{2}$$

have received very little attention from an analytical perspective [6, pp 53–5]. Until now, for example, the stability of flames involving even this relatively simple two-step mechanism has not been known. There are, in fact, quite a few radicals and other intermediate chemical species that serve mutually to catalyse their own production in the oxidation of hydrocarbons [6, 48], so that the model radical Z can be thought of as representing the overall effect of many energetic intermediate species in the form of a generic single 'radical' species.

A similar model that deserves mention [1] involves the non-branching production of an intermediate species

$$\begin{aligned} \mathrm{F} + \mathrm{M} \rightarrow \mathrm{Z} + \mathrm{M} \quad &: \quad k_{\mathrm{I}} = A_{\mathrm{I}} e^{-T_{\mathrm{I}}/T} \\ \mathrm{Z} + \mathrm{M} \rightarrow \mathrm{P} + \mathrm{M} \quad &: \quad k_{\mathrm{C}} = A_{\mathrm{C}} \end{aligned} \tag{3}$$

as an alternative for describing the kinetics of flames. This reaction scheme describes sequential chemical changes of the type $\mathrm{A} \rightarrow \mathrm{B} \rightarrow \mathrm{C}$ as have been used to study the effects of exothermic and endothermic stages in planar flames [2]. The first of the reactions in (3) is a simple fuel-decomposition step that serves a similar purpose to the first reaction in (2). However, in full hydrocarbon reaction schemes, individual elementary decomposition reactions tend to have extremely high activation temperatures and to be very slow indeed, so that the model (2) is likely to be a more realistic representative of the chemistry of most flames. Nevertheless, as a simple model in which the intermediate species is created without any self-catalysis, the scheme (3) is of interest and, as will be seen, it can be predicted to produce very similar forms of solution to those produced by the branching scheme (2).

Both of these relatively simple models are in need of deeper investigation. The main development beyond the one-step model is their thermally sensitive introduction of an intermediate energetic reactive species which typically serves both to provide a reservoir of chemical energy and to distribute the production of heat more widely than is possible with one-step kinetics, when the activation temperature T_{A} is large.

Of course, flames can also be modelled using detailed chemical schemes, and a great deal of work has been directed towards determining suitable chemical and transport models for hydrocarbon oxidation (see, e.g., [47–50]). Because of their enormous complexity these models can only realistically be studied numerically, as outlined in [50]. Calculations of this type are valuable in providing detailed information about the processes that operate inside flames. However, much more work will be needed before such studies can approach the same kind of understanding of the stability and dynamics of flames that has been possible through studying flames with one-step chemistry.

Another disadvantage of highly detailed and technically 'accurate' models is their lack of generality. By lumping processes together into more simple models, parameters such as Damköhler numbers, Lewis numbers and Zeldovich numbers arise naturally to 'approximate' the overall effects of reactivities, diffusivities, and so on, for a wide variety of possible combustible mixtures. For different choices of the parameters, these models can then be used to represent many types of flames and fuels at different mixture fractions, supplying a much more coherent overall picture.

Analytical solutions that depend on the parameters can then explain both relationships and differences between the behaviour of different types of flame much more readily, in terms of thresholds of bifurcation or instability that appear over readily identifiable ranges of the parameters. Numerous asymptotic as well as numerical studies based on one-step models of the type (1) have demonstrated this very clearly [1–13]. For example, the reason why stable flame balls must be non-adiabatic with a lean fuel having a low Lewis number was demonstrated in this way [29, 30]. In fact, until now, the stability of flame balls has not been demonstrated using any other form of model.

In this paper, we examine the structure and stability of flame balls modelled using either of the two-step reaction schemes (2) or (3), taking the chain-branching reaction $\mathrm{F} + \mathrm{Z} \rightarrow 2\mathrm{Z}$, or the radical-producing, fuel-decomposition reaction $\mathrm{F} + \mathrm{M} \rightarrow \mathrm{Z} + \mathrm{M}$, to produce no heat and to have a rate that depends sensitively on temperature. We therefore assume that T_{B}/T or T_{I}/T is large, where T_{B} is the activation temperature of the branching reaction in (2) and T_{I} is the activation temperature of the fuel decomposition reaction in (3); realistically, T_{B}/T is

likely to take a value between about five and ten for the slowest, and therefore rate-controlling, radical-branching reactions in hydrocarbon flames; although T_I/T is likely to be very much larger, reactant-decomposition reactions are simply too slow to play any significant role in real hydrocarbon combustion.

The model (3) is studied here for the sake of completeness and because it is easily found to generate almost the same kinds of flame structures as the model (2), demonstrating clearly that thermal sensitivity of the rate of production of radicals is the main factor that determines the structure and properties of the resulting flames. Finally, the completion reaction Z+M $\rightarrow$ P+M is taken to be exothermic and not thermally sensitive, having an activation temperature of zero.

The limits $T_B/T \rightarrow \infty$ or $T_I/T \rightarrow \infty$ lead to narrow reaction layers within which the fuel F is converted into the chemical radical Z. Jump conditions across this layer can be obtained, having some very significant differences from the corresponding conditions found for one-step chemistry. Both of the models (2) and (3) generate the same dimensionless jump conditions to leading order which, most notably, are found to be linear in all of the dependent variables and their gradients normal to the reaction sheet. These jump conditions can be used to model any form of premixed flame [41].

When applied to flame balls with heat loss, we find that multiple branches of solution arise; parts of the larger branch of solution are stable under some circumstances. Importantly, when sustained by the branching kinetic model (2), we also find numerically that this branch of solutions does not disappear as T_B/T is reduced to realistic values. Using the models studied here, the thermally sensitive production of an energetic intermediate reactive species does, therefore, provide a fully consistent asymptotic and numerical description of stable flame balls.

2. Model with chain branching kinetics

Taking the chain-branching reaction to release no heat in the reaction scheme (2), reactive–diffusive conservation equations for the absolute temperature $T(t, \mathbf{r})$, and the respective mass fractions $Y_F(t, \mathbf{r})$ and $Y_Z(t, \mathbf{r})$ of fuel and radical, become

$$\begin{aligned}
&\rho \partial_t Y_F = \rho D_F \nabla^2 Y_F - W_F \omega_B \\
&\rho \partial_t Y_Z = \rho D_Z \nabla^2 Y_Z + W_Z \omega_B - W_Z \omega_C \\
&\rho C_p \partial_t T = \lambda \nabla^2 T + Q\omega_C - \ell \\
&\omega_C = A_C \frac{\rho Y_Z}{W_Z} \frac{\rho}{W}, \qquad \omega_B = A_B \frac{\rho Y_F}{W_F} \frac{\rho Y_Z}{W_Z} e^{-T_B/T}
\end{aligned} \tag{4}$$

along with the boundary conditions

$$\lim_{|\mathbf{r}|\rightarrow\infty} (Y_F, Y_Z, T) = (Y_{F0}, 0, T_0)$$

in which, for simplicity, the density ρ, specific heat C_p, thermal conductivity λ, diffusivity of fuel D_F, diffusivity of the radical D_Z and the mean molecular weight W are all taken to be constant. The term ℓ represents the rate of heat loss to infinity through radiation. The molecular weights of fuel and radical are W_F and W_Z, respectively, and Q is the specific heat-release of the completion reaction. The pre-exponential factors in the rate expressions ω_B and ω_C for the branching and completion reactions in (2) are A_B and A_C, respectively.

If we now rescale the dependent and independent variables such that

$$t = t_s t', \qquad \mathbf{r} = r_s \mathbf{r}', \qquad T = T_0 + T_s T', \qquad Y_F = Y_{F0} F, \qquad Y_Z = Y_{Zs} Z$$

with

$$r_s^2 = \frac{t_s\lambda}{\rho C_p}, \qquad t_s = \frac{W}{\rho \mathrm{Le}_Z A_C}, \qquad \mathrm{Le}_F = \frac{\lambda}{\rho C_p D_F}, \qquad \mathrm{Le}_Z = \frac{\lambda}{\rho C_p D_Z}$$
$$Q' = \frac{QY_{F0}}{C_p T_s W_Z}, \qquad \ell' = \frac{\ell t_s}{\rho C_p T_s}, \qquad Y_{Zs} = \frac{\mathrm{Le}_Z W_Z}{\mathrm{Le}_F W_F} Y_{F0} \tag{5}$$
$$\beta^2 e^{T_B/(T_0+T_s)} = \frac{A_B W}{A_C W_F} Y_{F0}, \qquad \beta = \frac{T_B T_s}{(T_0+T_s)^2}, \qquad q = \frac{T_s}{T_0+T_s}$$

then (after dropping the primes) a dimensionless version of the problem can be written as

$$\begin{aligned} \mathrm{Le}_F F_t &= \nabla^2 F - \beta^2 F Z k(T) \\ \mathrm{Le}_Z Z_t &= \nabla^2 Z - Z + \beta^2 F Z k(T) \\ T_t &= \nabla^2 T + \frac{QZ}{\mathrm{Le}_F} - \ell \\ k(T) &= \exp\left(\beta \frac{T-1}{1+q(T-1)}\right) \end{aligned} \tag{6}$$

with the boundary condition

$$\lim_{|\mathbf{r}|\to\infty} (T, F, Z) = (0, 1, 0). \tag{7}$$

The non-dimensionalization thus serves to define natural time and length scales for the rates of heat production and heat conduction, while the diffusivities of fuel and radical are then measured by the inverses of their respective Lewis numbers Le_F and Le_Z. The dimensionless function $F(t, \mathbf{r})$ measures the mass fraction of the fuel F, scaled against its value at infinity, while the function $Z(t, \mathbf{r})$ measures the mass fraction of the radical Z, scaled so as to balance the rates of diffusion and either production or consumption of fuel and radical, respectively, due to the chain-branching reaction. The dimensionless heat of reaction Q represents the chemical enthalpy of the mixture at infinity and the term ℓ represents the dimensionless rate of radiative heat loss, both scaled against the change in thermal enthalpy that occurs if the dimensional temperature changes by the scale factor T_s. The latter scale factor is used to define the new dimensionless temperature scale $T(t, \mathbf{r})$, the origin of which is chosen, naturally enough, to be the temperature at infinity.

The choice of the scale factor T_s deserves more detailed discussion; it is clearly chosen so that the dimensionless temperature $T = 1$ occurs at an absolute dimensional reference temperature of $T_0 + T_s$. It can be noted, in passing, that the Zeldovich number β, as defined in (5), differs from the definition of the Zeldovich number that is relevant for flames that are modelled using one-step chemistry; rather than being based on the adiabatic flame temperature or, in the case of flame balls, the maximum adiabatic flame-ball temperature, it is based on the reference temperature $T_0 + T_s$. The exponent in the dimensionless rate constant $k(T)$ then linearizes to $\beta(T - 1)$ about the dimensionless temperature $T = 1$ or, equivalently, the dimensional reference temperature $T_0 + T_s$. Correspondingly, q measures the ratio of the temperature change to the absolute temperature only up to $T_0 + T_s$, rather than the adiabatic maximum temperature.

It can also be noted in passing that, if Y_F is held fixed at Y_{F0}, then the dimensional temperature $T_0 + T_s$ is the temperature at which $\omega_B = \beta^2 \omega_C$. This temperature is higher than the temperature at which we would find $\omega_B = \omega_C$.

The absolute temperature T_c at which the rates of the branching and completion reactions are the same, that is $\omega_B = \omega_C$, is known as the 'crossover temperature' ([6, 22] and [7, p 27]). At this temperature, in a spatially homogeneous system, the rate of chain-branching radical production exactly balances its loss rate through the completion reaction, since there are

no diffusive losses. At temperatures above T_c, for which $\omega_B > \omega_C$ with $Y_F = Y_{F0}$, the homogeneous form of the model (6) gives

$$\mathrm{Le}_Z \frac{\mathrm{d}Z}{\mathrm{d}t} = \left(\beta^2 F k(T) - 1\right) Z$$

with the coefficient $\beta^2 F k(T) - 1$ being positive if $F = 1$. Given any small non-zero initial radical concentration, it follows that an exponential chain-branching growth in the radical concentration would occur until sufficient fuel is used up to reduce the coefficient to zero; the radical concentration $Z = 0$ would thus represent an unstable equilibrium of the homogeneous system. Conversely, at temperatures below the crossover temperature T_c, the sign of $\beta^2 F k(T) - 1$ becomes negative and $Z = 0$ then represents a stable equilibrium of the homogeneous system; any non-zero initial value for Z decreases exponentially with time. Unlike the one-step kinetic model (1), the branching model scheme (2) does not therefore suffer from the cold-boundary difficulty [1], provided the fresh-gas temperature is below the crossover temperature.

The reference temperature $T_0 + T_s$ must be chosen to be higher than the crossover temperature T_c so that, at this temperature, we would have $\omega_B = \beta^2 \omega_C$ if Y_F is held fixed at Y_{F0}. The extra factor of β^2 that appears in the dimensionless chain-branching rate-expression $\beta^2 F Z k(T)$ in the model (6) reflects the fact that the chain-branching production of radicals, at the dimensionless temperature $T = 1$, must now compete with the diffusive removal of radicals which will be seen to be a significantly stronger effect than the removal of radicals by the completion reaction. Also, the consumption of fuel by the branching reaction tends to reduce considerably the value of F whenever temperatures reach the reference temperature, as will be seen.

Reduced-chemistry studies of methane flames, such as [20–22], suggest that the reference temperature $T_0 + T_s$, at which the fuel concentration will be seen to decrease towards zero, has a value of roughly 1300 K under atmospheric conditions (see [22]). Taking, for example, the activation temperature of 8500 K, for the key chain-branching reaction $H + O_2 \rightarrow OH + O$, to represent T_B and taking T_0 to be room temperature (about 300 K) then leads an estimate for the Zeldovich number of $\beta \approx 5$. Solving the equation $\beta^2 k(T) - 1 = 0$, with $q = \frac{1000}{1300}$, then leads to an estimate for the crossover temperature of $T_c \approx 900$ K. The independent arguments of Liñán and Williams [6, pp 53–5], Warnatz *et al* [50, pp 104–6] or Westbrook [48, 49] seem to indicate that a realistic crossover temperature should indeed be approximately 850–900 K, suggesting that a typical value of β for hydrocarbons might indeed be about five. Even though this is not particularly large, we shall use the limit $\beta \rightarrow \infty$ to construct asymptotic solutions of (6) and (7), using subsequent numerical calculations to examine how solutions might change for finite values of β.

The overall relationship between T_0, T_s, T_c, T_B and β can be written in the form

$$\frac{(T_0 + T_s)^2}{T_s T_c} = \frac{T_0 + T_s}{T_s} + \frac{\ln \beta^2}{\beta}, \qquad \beta = \frac{T_B T_s}{(T_0 + T_s)^2} \tag{8}$$

which, if T_0 and T_c are held fixed, can be used to solve for the scale factor T_s in terms of either β or T_B. In the case for which T_c is assigned the realistic value of $T_c = 900$ K, figure 1 shows how the reference temperature $T_0 + T_s$ varies as a function of β at a number of different far-field temperatures $T_0 < T_c$. In all cases, the reference temperature approaches the crossover temperature as $\beta \rightarrow \infty$ (or, equivalently $T_B \rightarrow \infty$).

In the leading-order asymptotic description (that will be presented in section 4) it may be best therefore to think of the dimensionless temperature $T = 1$ as being more-or-less the same as the dimensional crossover temperature T_c. Dimensional temperatures must increase above T_c if there is going to be any significant level of chemical activity at all. The higher

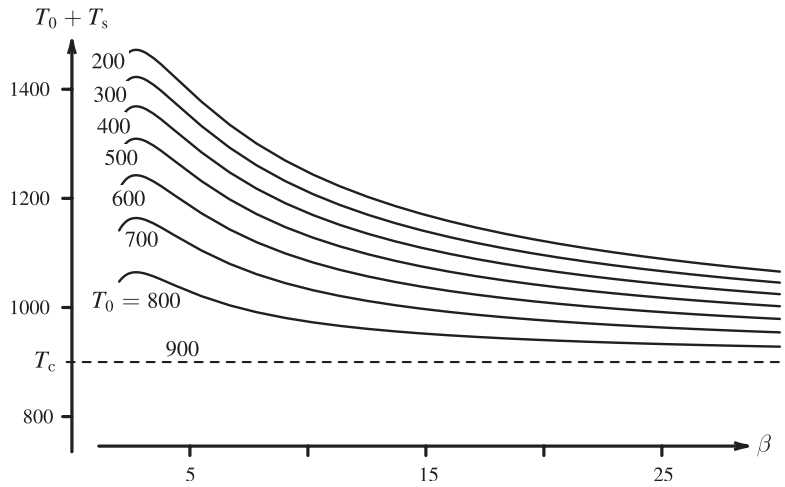

Figure 1. The reference absolute temperature $T_0 + T_s$ as a function of the Zeldovich number β for various far-field temperatures T_0 at a fixed value of $T_c = 900$ K for the crossover temperature.

order asymptotic description (presented next, in section 2.1) shows that the activity becomes stronger and leads to a narrow region of branching reaction if the temperature rises through $T_0 + T_s$. Nearly all branching activity takes place between the two temperatures T_c and $T_0 + T_s$, with fuel leakage occurring if temperature has a maximum value that is closer to T_c.

Finally, eliminating all of the reaction-rate terms in (6) yields another equation

$$\partial_t \left(\mathrm{Le_F} F + \mathrm{Le_Z} Z + \frac{T \, \mathrm{Le_F}}{Q} \right) = \nabla^2 \left(F + Z + \frac{T \, \mathrm{Le_F}}{Q} \right) - \frac{\ell \, \mathrm{Le_F}}{Q}$$

which could be used to replace any one of the other conservation equations in (6). The time derivative term of this equation can be used to show that the adiabatic planar flame temperature, at which $F = Z = 0$ with $\ell \equiv 0$, is $T = Q$, while the Laplacian term shows that the temperature of steady adiabatic fully-reacted flame balls is $T = Q/\mathrm{Le_F}$. In studying flame balls it is convenient therefore to define

$$\tilde{Q} = \frac{Q}{\mathrm{Le_F}}$$

to replace $Q/\mathrm{Le_F}$ in the dimensionless model (6).

2.1. Narrow region of chain-branching reaction

For $\beta \gg 1$, if T increases through unity, then the temperature-sensitive non-linear Arrhenius factor $k(T)$ changes rapidly from small to large values, implying that a narrow reactive boundary layer must exist around $T = 1$. There are two situations, with differing forms of solution, which depend on whether or not there is a maximum value of temperature near $T = 1$.

Readers who are not particularly interested in the details of the asymptotic structure of this narrow reaction region, or the details of the model (3) with fuel decomposition that will be described in section 3, can skip to section 4 where the resulting overall leading order flame-sheet model is presented and analysed.

2.1.1. Temperature increasing through unity. Supposing that there is an interface $\mathbf{r} = \mathbf{R}(r_1, r_2)$, parameterized by two scalar variables r_1 and r_2, which follows a thin region of

reaction with unit normal $\hat{\mathbf{n}}$, then rescaling such that

$$T = 1 + \beta^{-1}s, \qquad \mathbf{r} = \mathbf{R} + \hat{\mathbf{n}}\,\beta^{-1}\eta, \qquad Z = \bar{Z} + \beta^{-1}\xi, \qquad F = \beta^{-1}f \tag{9}$$

gives rise to the leading order inner equations for f, ξ and s

$$f_{\eta\eta} = \bar{Z} f e^{s} = -\xi_{\eta\eta}, \qquad s_{\eta\eta} = 0. \tag{10}$$

Thus, by choosing the value of $\bar{Z}$ so that $f + \xi = 0$ when $\eta = 0$, we can deduce that

$$s = s_0 + \mu\eta, \qquad f + \xi = \nu\eta$$

for constants μ, ν and s_0.

Provided $\mu \neq 0$, so that the temperature T actually does change through unity, the problem can be written as

$$\mu^2 f_{ss} = \bar{Z} f e^{s} \quad \text{or} \quad \zeta \frac{\mathrm{d}^2 f}{\mathrm{d}\zeta^2} + \frac{\mathrm{d}f}{\mathrm{d}\zeta} - 4\zeta f = 0 \qquad \text{with } \mu^2\zeta^2 = \bar{Z}e^{s}$$

leading to the solution (after imposing a physically necessary condition of chemical equilibrium or $f \to 0$, in the limit as $s \to \infty$)

$$\begin{aligned} f &= A\mathrm{K}_0(2\zeta) = A\mathrm{K}_0\left(\frac{-2\bar{Z}^{1/2}e^{s/2}}{\mu}\right) \\ &= A \times \begin{cases} \mathrm{O}\left(e^{-s/2}\exp\left(\dfrac{-2\bar{Z}^{1/2}e^{s/2}}{\mu}\right)\right) & \text{as } s \to \infty \\ -\frac{1}{2}s - \gamma + \ln\left(\dfrac{\mu}{\bar{Z}^{1/2}}\right) + \mathrm{O}(se^{s}) & \text{as } s \to -\infty \end{cases} \end{aligned}$$

for any constant A, where K_0 is a modified Bessel's function of order zero and γ is Euler's constant ($\gamma \approx 0.577\,216$).

To leading order, when $|s|$ or $|\eta|$ is large, this gives the asymptotic behaviour of the scaled fuel concentration f, and the perturbation ξ in the radical concentration, as

$$f = \nu\eta - \xi = A \times \begin{cases} 0 & \text{as } \mu\eta \to \infty \\ -\frac{1}{2}(s_0 + \mu\eta) - \gamma + \ln\left(\dfrac{\mu}{\bar{Z}^{1/2}}\right) & \text{as } \mu\eta \to -\infty. \end{cases}$$

By choosing the exact location of the interface $\mathbf{R}$ (the origin of η) such that these two asymptotic forms of behaviour of f for large $|\eta|$ extrapolate back to intersect at $\eta = 0$, we find that $s_0 = \ln(\mu^2/\bar{Z}) - 2\gamma$.

The conditions for matching the behaviour of these inner solutions, at large η, with outer solutions, as $\mathbf{r} \to \mathbf{R}^{\pm}$, then becomes

$$\begin{aligned} &[F_n] + [Z_n] = [T_n] = [T] = [F] = [Z] = F = 0 \\ &T = 1 + \beta^{-1}\left(\ln\frac{T_n^2}{Z} - 2\gamma\right) \end{aligned} \tag{11}$$

at $\mathbf{r} = \mathbf{R}^{\pm}$, provided $T_n \neq 0$ at the interface. In addition, we must have $F = 0$ where $T > 1$ and if we were to have, for example, $F = 0$ for $n < 0$ and $F > 0$ for $n > 0$, then we must also have that $T_n < 0$. The subscript n in these jump conditions denotes the partial derivative or gradient in the direction normal to the interface and the square brackets $[\cdot]$ represent the value of the contents of the brackets on the side to which $\hat{\mathbf{n}}$ points minus the value on the opposite side.

This asymptotic result fails at some stage if $|T_n|$ becomes too small. It is worth noting that, for large values of β, either equation (8) or the relation $\beta^2 k(T) = 1$ can be used to show that the dimensionless value of the crossover temperature is given by $T \sim 1 - 2\beta^{-1}\ln\beta$.

It follows that, if T_n decreases to the order of β^{-1} the temperature predicted in (11) is then virtually the same as the crossover temperature. At such small values of T_n, the asymptotic estimate in (11) for the value of T at the flame sheet is no longer valid. Instead, it is necesary to focus attention on a local maximum of temperature that will be seen to be below the reference temperature $T = 1$.

2.1.2. Maximum temperature near unity. If temperature has a maximum value, so that T_n would then be small in the region where the branching reaction is active, we can note that the value of $\nabla^2 T$ or T_{nn} should then be of order one and negative. In such a situation, a different inner rescaling is appropriate. A suitable scaling for the inner problem is

$$\begin{aligned} T &= 1 + \beta^{-1}\big(s - \tfrac{3}{2}\ln\beta\big), \qquad & \mathbf{r} &= \mathbf{R} + \hat{\mathbf{n}}\,\beta^{-1/2}\eta \\ Z &= \bar{Z} + \beta^{-1/2}\xi, & F &= \bar{F} + \beta^{-1/2} f. \end{aligned} \tag{12}$$

It can be noted that order one values of the inner temperature gradient s_η then correspond to outer temperature gradients T_n that are of the order of $\beta^{-1/2}$.

The scalings (12) lead to the leading order inner equations for f, ξ and s

$$f_{\eta\eta} = \bar{F}\bar{Z}e^{s} = -\xi_{\eta\eta}, \qquad s_{\eta\eta} = \bar{\ell} - \tilde{Q}\bar{Z}$$

with $\bar{\ell}$ being a constant approximation to ℓ in the thin reaction zone. Since s must be taken to have a local maximum, it can be noted that we must have $\bar{\ell} < \tilde{Q}\bar{Z}$. Thus, the rate of heat production must exceed the rate of heat loss near the maximum in temperature. (Similar results would arise even if ℓ varied significantly with η, as long as $\tilde{Q}\bar{Z} - \ell$ is greater than some positive quantity for all order one values of η. This ensures that s decreases without bound both as $\eta \to \infty$ and as $\eta \to -\infty$).

With $\mathbf{R}$ and $\bar{F} + \bar{Z}$ being chosen suitably we then have

$$s = s_0 - \tfrac{1}{2}(\tilde{Q}\bar{Z} - \bar{\ell})\eta^2, \qquad f + \xi = \nu\eta$$

leading to

$$f_{\eta\eta} = \bar{F}\bar{Z}e^{s_0}e^{-(\tilde{Q}\bar{Z}-\bar{\ell})\eta^2/2}$$

with the solution, for a suitable normalization of the value of $\bar{F}$

$$f = \eta f_\eta^- + \bar{F}\bar{Z}e^{s_0}\sqrt{\frac{\pi/2}{\tilde{Q}\bar{Z}-\bar{\ell}}}\,\eta\,\mathrm{erfc}\left(-\eta\sqrt{\tfrac{1}{2}(\tilde{Q}\bar{Z}-\bar{\ell})}\right) + \frac{\bar{F}\bar{Z}e^{s_0}}{\tilde{Q}\bar{Z}-\bar{\ell}}e^{-(\tilde{Q}\bar{Z}-\bar{\ell})\eta^2/2}$$

where $f_\eta^\pm$ is the limit of f_η as $\eta \to \pm\infty$. It can be seen that

$$[f_\eta] = f_\eta^+ - f_\eta^- = \bar{F}\bar{Z}e^{s_0}\sqrt{\frac{2\pi}{\tilde{Q}\bar{Z}-\bar{\ell}}} \qquad \text{or} \qquad s_0 = \ln\frac{[f_\eta]}{\bar{F}\bar{Z}} + \tfrac{1}{2}\ln\frac{\tilde{Q}\bar{Z}-\bar{\ell}}{2\pi}.$$

Matching conditions for the outer problem, at $\mathbf{r} = \mathbf{R}^\pm$, that result from this solution, are now

$$\begin{aligned} &[F_n]{+}[Z_n] = [T] = [F] = [Z] = T_n = 0 \\ &T = 1{+}\beta^{-1}\left(\ln\frac{[F_n]}{FZ}{+}\tfrac{1}{2}\ln\frac{\tilde{Q}Z-\ell}{2\pi} - \tfrac{3}{2}\ln\beta\right) \end{aligned} \tag{13}$$

which fails at some stage if F becomes too small at the interface. The same kind of result would be found even if ℓ varied significantly with η, as long as the scaled temperature s has a local maximum near $\eta = 0$. The value of ℓ in (13), at $\mathbf{r} = \mathbf{R}$, may then need to be defined differently, as a suitable average, but the overall effect would be much the same.

It can be noted that if F becomes of the order of β^{-1}, as it is in the scalings (9) that are relevant for temperatures that increase through unity, then the temperature that the conditions (13) predict at the interface increases to $T \sim 1 - \frac{1}{2}\beta^{-1}\ln\beta$. Otherwise, the temperature at the interface satisfies $T \sim 1 - \frac{3}{2}\beta^{-1}\ln\beta$ which is closer to, but still greater than, the crossover temperature.

In general, if temperature has a local maximum at the reaction sheet then the reactant concentration F need not be zero on either side of it. That is, reactant can survive through the reaction sheet in a way that it cannot do if $T_n \neq 0$ at the sheet.

3. Model with fuel decomposition

Taking the fuel decomposition reaction to release no heat in the reaction scheme (3), dimensional reactive–diffusive conservation equations become

$$\begin{aligned}
&\rho\partial_t Y_{\mathrm{F}} = \rho D_{\mathrm{F}}\nabla^2 Y_{\mathrm{F}} - W_{\mathrm{F}}\,\omega_{\mathrm{I}}\\
&\rho\partial_t Y_{\mathrm{Z}} = \rho D_{\mathrm{Z}}\nabla^2 Y_{\mathrm{Z}} + W_{\mathrm{Z}}\omega_{\mathrm{I}} - W_{\mathrm{Z}}\omega_{\mathrm{C}}\\
&\rho C_{\mathrm{p}}\,\partial_t T = \lambda\nabla^2 T + Q\omega_{\mathrm{C}} - \ell\\
&\omega_{\mathrm{C}} = A_{\mathrm{C}}\,\frac{\rho Y_{\mathrm{Z}}}{W_{\mathrm{Z}}}\,\frac{\rho}{W}, \qquad \omega_{\mathrm{I}} = A_{\mathrm{I}}\frac{\rho Y_{\mathrm{F}}}{W_{\mathrm{F}}}\,\frac{\rho}{W}\,e^{-T_{\mathrm{I}}/T}
\end{aligned}$$

in which ω_{I} is the rate expression for the fuel decomposition reaction in (3) with pre-exponential factor A_{I}. All other terms have the same meaning as in the model (4).

In fact, these equations are very similar to the equation (4) that describe a chain-branching reaction process, and they can be made dimensionless in a very similar way; the only changes that are needed from the reference scalings (5) are the new implicit definitions for β and T_{s}

$$\beta^2 e^{\,T_{\mathrm{I}}/(T_0+T_{\mathrm{s}})} = \frac{A_{\mathrm{I}}W_{\mathrm{Z}}Y_{\mathrm{F0}}}{A_{\mathrm{C}}W_{\mathrm{F}}Y_{\mathrm{Zs}}}, \qquad \beta = \frac{T_{\mathrm{I}}T_{\mathrm{s}}}{(T_0+T_{\mathrm{s}})^2}$$

to produce the dimensionless version of the model

$$\begin{aligned}
&\mathrm{Le}_{\mathrm{F}}F_t = \nabla^2 F - \beta^2 F k(T)\\
&\mathrm{Le}_{\mathrm{Z}}Z_t = \nabla^2 Z - Z + \beta^2 F k(T)\\
&T_t = \nabla^2 T + \tilde{Q}Z - \ell\\
&k(T) = \exp\left(\beta\frac{T-1}{1+q(T-1)}\right).
\end{aligned} \tag{14}$$

The only difference from the dimensionless model (6), with $\tilde{Q}$ replacing $Q/\mathrm{Le}_{\mathrm{F}}$, is the disappearance of a factor Z from the radical-producing reaction rate $\beta^2 F k(T)$. The new definition of β differs from the corresponding definition in (5) only because the activation temperature T_{I} of the fuel-decomposition reaction in (3) replaces T_{B}.

Unlike the chain-branching model, an unreacted state with $Z = 0$ is not stable at any low enough temperature. In fact, there is no crossover temperature for this model. However, in direct analogy with the chain-branching model, the dimensional reference temperature $T_0 + T_{\mathrm{s}}$ is the temperature at which $\omega_{\mathrm{I}} = \beta^2\omega_{\mathrm{C}}$ with Y_{F} held fixed at Y_{F0} and Y_{Z} held fixed at Y_{Zs}. The activation temperatures of both of the main fuel-decomposition reaction-steps, $CH_4 + M \rightarrow CH_3 + H + M$ and $H_2 + M \rightarrow 2H + M$, for methane and hydrogen are about 53 000 K, suggesting that β might have a value of about 30 or more, if $T_0 + T_{\mathrm{s}}$ is a temperature found in any typical hydrocarbon flame, that is, a temperature that is less than about 2000 K. One fuel and oxidant decomposition reaction $CH_4 + O_2 \rightarrow CH_3 + HO_2$ has an activation temperature of 28 200 K, suggesting that an effective Zeldovich number could be as low as about $\beta = 12$.

It must be remembered that decomposition reactions are, in reality, almost completely insignificant in most hydrocarbon combustion, where chain-branching or chain-propagation reactions are mainly responsible for the conversion of reactants to radicals [1, 6]. On the other hand, in other chemical systems the model may be more relevant [2] and, as mathematical models, it will soon be seen that both of the reaction schemes (2) and (3) lead to the same leading-order dimensionless solutions if $\beta \gg 1$. This fact serves to stress the general nature of the resulting matched asymptotic picture.

3.1. Narrow region of chain-branching reaction

Because the dimensionless model (14) is very similar to the model (6), the structure of the inner reaction region with $\beta \gg 1$, in which F is consumed when T is near unity, is also very similar. Readers who are not interested in the details can skip to section 4.

3.1.1. Temperature increasing through unity. Exactly the same scalings (9) can be applied, to arrive at the leading order inner equations for f, ξ and s

$$f_{\eta\eta} = f e^{s} = -\xi_{\eta\eta}, \qquad s_{\eta\eta} = 0.$$

The only difference between these equations and (10) is the disappearance of the factor $\bar{Z}$. Exactly the same arguments can therefore be applied, with $\bar{Z}$ replaced by unity, to arrive at the conditions for matching with outer asymptotic solutions, at $\mathbf{r} = \mathbf{R}^{\pm}$

$$\begin{aligned} &[F_n] + [Z_n] = [T_n] = [T] = [F] = [Z] = F = 0 \\ &T = 1 + \beta^{-1}\left(\ln T_n^2 - 2\gamma\right) \end{aligned} \tag{15}$$

provided $T_n \neq 0$ at the interface.

3.1.2. Maximum temperature near unity. If the temperature has a maximum value near unity, the scaling (12) can be used to arrive at the leading order inner equations for f, ξ and s

$$f_{\eta\eta} = \bar{F} e^{s} = -\xi_{\eta\eta}, \qquad s_{\eta\eta} = \bar{\ell} - \tilde{Q}\bar{Z}$$

with the analysis following in exactly the same way to lead to the equation for f

$$f_{\eta\eta} = \bar{F} e^{s_0} e^{-(\tilde{Q}\bar{Z} - \bar{\ell})\eta^2/2}$$

in which the factor $\bar{F}$ is not multiplied by $\bar{Z}$. The solution again parallels the solution for chain-branching chemistry, with $\bar{F}\bar{Z}$ replaced by $\bar{F}$, to arrive at the matching conditions for the outer problem, at $\mathbf{r} = \mathbf{R}^{\pm}$

$$\begin{aligned} &[F_n] + [Z_n] = [T] = [F] = [Z] = T_n = 0 \\ &T = 1 + \beta^{-1}\left(\ln\frac{[F_n]}{F} + \tfrac{1}{2}\ln\frac{\tilde{Q}Z - \ell}{2\pi} - \tfrac{3}{2}\ln\beta\right). \end{aligned} \tag{16}$$

As before, the value of ℓ, at $\mathbf{r} = \mathbf{R}$ in these conditions, might have to be expressed as some suitable average of ℓ if it changes significantly through the reaction region.

4. Leading-order reaction-sheet model

Taking β to be infinitely large, all of these forms of jump condition can be combined into one form that deals with all cases. A leading-order model that treats either the chain branching or

the fuel decomposition reaction as occurring at an infinitesimally thin reaction sheet at $\mathbf{r} = \mathbf{R}$ is now, for $\mathbf{r} \neq \mathbf{R}$

$$\begin{aligned} T_t &= \nabla^2 T + \tilde{Q} Z - \ell \\ \mathrm{Le_F} F_t &= \nabla^2 F \\ \mathrm{Le_Z} Z_t &= \nabla^2 Z - Z. \end{aligned} \tag{17}$$

In addition, we must have $F \equiv 0$ where $T > 1$. The leading-order jump conditions to be applied across the interface at $\mathbf{r} = \mathbf{R}^{\pm}$ become, simply

$$[F_n] + [Z_n] = [T_n] = [T] = [F] = [Z] = T - 1 = F T_n = 0 \tag{18}$$

where, as usual, the subscript n represents the gradient of a quantity in the normal direction, that is $\partial_n = \hat{\mathbf{n}} \cdot \nabla$, where $\hat{\mathbf{n}}$ is a unit normal to the interface. The notation $[\cdot]$ denotes the jump in the value of a quantity across the interface, being equal to the value of the content of the square brackets on the side to which $\hat{\mathbf{n}}$ points minus its value on the opposite side.

If the temperature T exceeds unity on one side of the reaction sheet, so that $T_n \neq 0$, then F must be set to zero at the reaction sheet. On the other hand, if the temperature has a local maximum of unity at the reaction sheet, so that $T_n = 0$, then the value of F need not be set to zero. Thus, this set of conditions deals with both types of inner problem examined above, for each type of reaction scheme, at least to leading order as $\beta \to \infty$. The jump conditions (11) and (13) or (15) and (16) are in fact valid to higher order in β^{-1} so that it would be possible to develop more precise descriptions, offering relatively minor corrections to the leading order description when β is large.

Apart from the condition $F T_n = 0$, a notable feature of the leading order jump conditions (18), as $\beta \to \infty$, is that they are entirely linear in F, Z, T and their normal derivatives. The condition $F T_n = 0$ is equivalent to having either $F = 0$ or $T_n = 0$ which, taken separately, are also linear conditions to be applied at the interface. Only one of the jump conditions is linear and inhomogeneous, namely $T - 1 = 0$.

The remaining conditions in (18) state that the temperature, the mass fractions of fuel and radical and the temperature gradient must all be continuous across the reaction sheet, where the temperature also has the value $T = 1$. Also, the jump in the normal gradient of the dimensionless fuel mass fraction is exactly equal and opposite to the jump in the normal gradient of the dimensionless mass fraction of the radical. This condition amounts to the natural requirement that the flux of fuel molecules into the interface must exactly balance the flux of radical molecules out of the interface.

4.1. Reaction-sheet model for a spherical flame ball with linear heat loss

With spherical symmetry, the reaction sheet can be taken to lie at a radius $r = R(t)$ from a centre of symmetry, at $r = 0$. If we also model the heat loss term such that $\ell = a^2 T$, representing heat losses that are linear in temperature, then the problem satisfies the equations for $r \neq R(t)$

$$\begin{aligned} T_t &= \left(\partial_{rr} + 2r^{-1}\partial_r\right) T + \tilde{Q} Z - a^2 T \\ \mathrm{Le_F} F_t &= \left(\partial_{rr} + 2r^{-1}\partial_r\right) F \\ \mathrm{Le_Z} Z_t &= \left(\partial_{rr} + 2r^{-1}\partial_r\right) Z - Z \end{aligned} \tag{19}$$

taking $F \equiv 0$ where $T > 1$, along with the jump conditions at $r = R^{\pm}$

$$[F_r] + [Z_r] = [T_r] = [T] = [F] = [Z] = T - 1 = F T_r = 0. \tag{20}$$

In the far field, as $r \to \infty$, the boundary conditions to be satisfied are

$$\lim_{r \to \infty} (T, F, Z) = (0, 1, 0). \tag{21}$$

Several studies of flame balls using one-step kinetics have considered the relative importance and differing effects of non-linear radiative heat losses and linear heat losses, for example [30, 38] and [44–46]. In dimensional terms, Stefan's law would give a rate of heat loss that is proportional to $T^4 - T_0^4$, which includes a linear component of $4(T - T_0)T_0^3$ while it also has a maximum value of the order of $(T_0 + T_s)^4$. If $T_s \approx 1000\,\mathrm{K}$ and $T_0 \approx 300\,\mathrm{K}$, this maximum value should therefore be roughly 30 times greater than the linear heat loss component within the region where the absolute temperature is of the order of $T_0 + T_s$. Non-linear radiative terms might therefore seem to be overwhelmingly stronger than their linear component.

However, the volume of the hottest region is approximately $\frac{4}{3}\pi R^3$ while, if overall heat losses are weak so that $T \approx T_0 + T_s R/r$ [28], the volume of the region in which absolute temperatures are about, say, $\frac{5}{4}T_0$ (where linear heat losses occur at a rate of about T_0^4) is very much larger, at the order of $\frac{4}{3}\pi(4RT_s/T_0)^3$. Linear heat losses are of course higher than T_0^4 at smaller values of r, but as a rough underestimate, the full volumetric effect of these linear 'far field' heat losses is therefore a factor of about five or more times greater than those of the fully non-linear losses in the hottest region. Thus, even though temperatures are low in the far field, the overall effect of the linear component of heat losses can significantly exceed that of non-linear radiative losses. Moreover, these linear losses are still radiative in orgin.

A number of studies of flame balls with one-step chemistry have uncovered significant effects that are mainly due to such linear volumetric heat losses, for example [30, 39]. Strain and shear in the flow field around a flame ball serve to draw cold gases closer to the flame ball and to advect hot gases away from it. In a sense therefore, non-uniform flows also serve to induce effective heat losses, in a way that increases with the size of a flame ball, and these too have been shown to provide a stabilizing effect [34, 36, 40]. Heat losses through a cold boundary at a finite distance have the same overall effect [35]. The evidence provided by these studies demonstrates that it is more the existence of heat losses and the way in which they vary with the size of a flame ball, rather than the details of their cause, that stabilizes the flame ball. Also, volumetric 'far field' losses, which are weak and effectively linear seem to be at least as important as, and possibly much more important than, non-linear high-temperature losses.

As well as its being a significant and possibly dominating effect, adopting a linear heat-loss law is also very useful in the model equations (19) because it preserves the linearity of the problem. Indeed, with the exception of the condition $FT_n = 0$, which of course is equivalent to two alternative linear conditions, the entire problem (19)–(21) then represents a linear free boundary problem.

We shall now examine this model to determine the structure and stability of spherically symmetric flame balls involving the chain-branching chemical scheme (2) with heat losses that are linear in temperature.

5. Structure and stability of steady flame balls

5.1. Steady solutions

Considering only steady cases, for which $\partial_t \equiv 0$ and $R \equiv \bar{R}$, the equations to be satisfied are

$$\begin{aligned} 0 &= \left(\partial_{rr} + 2r^{-1}\partial_r\right) T + \tilde{Q}Z - a^2 T \\ 0 &= \left(\partial_{rr} + 2r^{-1}\partial_r\right) F \\ 0 &= \left(\partial_{rr} + 2r^{-1}\partial_r\right) Z - Z \end{aligned} \tag{22}$$

taking $F \equiv 0$ where $T > 1$, along with the jump conditions (20) and boundary conditions (21). Solutions of these linear ordinary differential equations are not difficult to find. The solution,

for $a \neq 1$, already satisfying the boundary conditions (21) at infinity and most of the conditions (20), can be written as

$$F = F_0(r) = \begin{cases} 1 - \dfrac{(1-\bar{F})\bar{R}}{r} & \text{for } r > \bar{R} \\ \bar{F} & \text{for } r < \bar{R} \end{cases}$$

$$Z = Z_0(r) = \frac{(1-\bar{F})/r}{1+\coth\bar{R}} \begin{cases} e^{\bar{R}-r} & \text{for } r > \bar{R} \\ \dfrac{\sinh r}{\sinh\bar{R}} & \text{for } r < \bar{R} \end{cases} \tag{23}$$

$$T = T_0(r) = -\frac{\tilde{Q}Z_0(r)}{1-a^2} + \frac{\tilde{Q}/a}{1-a^2}\,\frac{(1-\bar{F})/r}{1+\coth(a\bar{R})} \begin{cases} e^{a(\bar{R}-r)} & \text{for } r > \bar{R} \\ \dfrac{\sinh(ar)}{\sinh(a\bar{R})} & \text{for } r < \bar{R}. \end{cases}$$

If $a = 1$ then the solution for T is given by the non-singular limit as $a \to 1$, namely

$$T = T_0(r) = \tfrac{1}{2}\tilde{Q}\frac{(1-\bar{F})/r}{1+\coth\bar{R}} \begin{cases} (1-\bar{R}\coth\bar{R}+r)e^{\bar{R}-r} & \text{for } r > \bar{R} \\ \dfrac{(1+\bar{R})\sinh r - r\cosh r}{\sinh\bar{R}} & \text{for } r < \bar{R}. \end{cases}$$

In this solution, all of the conditions $[F_r] + [Z_r] = [T_r] = [T] = [F] = [Z] = 0$ are satisfied at $r = \bar{R}^{\pm}$, leaving only the conditions $FT_r = 0$ and $T - 1 = 0$ to be imposed.

Since $(\mathrm{d}/\mathrm{d}\bar{R})[(\bar{R}+1)/(1+\coth\bar{R})]$ is positive and less than unity for all $\bar{R} > 0$, we can note that the temperature gradient at $r = \bar{R}$

$$T_0'(\bar{R}) = \frac{\tilde{Q}(1-\bar{F})}{\bar{R}^2(1-a^2)a}\left(a\frac{\bar{R}+1}{1+\coth\bar{R}} - \frac{a\bar{R}+1}{1+\coth(a\bar{R})}\right) \tag{24}$$

must be negative for all values of $\bar{F} < 1$, $\bar{R} > 0$ and $a > 0$, including its limit as $a \to 1$. It follows from the condition that $FT_r = 0$, at $r = \bar{R}$, that we must have

$$\bar{F} = 0.$$

The only remaining condition, that $T = 1$ at $r = \bar{R}$, finally gives

$$T_0(\bar{R}) = \frac{\tilde{Q}}{\bar{R}(1-a^2)}\left(\frac{1}{a+a\coth(a\bar{R})} - \frac{1}{1+\coth\bar{R}}\right) = 1.$$

Solutions are therefore determined by the implicit equation for a and $\bar{R}$ at fixed values of $\tilde{Q}$

$$\bar{R} = \frac{\tilde{Q}}{1-a^2}\left(\frac{1}{a+a\coth(a\bar{R})} - \frac{1}{1+\coth\bar{R}}\right). \tag{25}$$

We can also note, for later use, that at $r = \bar{R}$

$$[T_0'] = [T_0''] = 0, \qquad F_0'(\bar{R}^+) = [F_0'] = \frac{1}{\bar{R}} = -[Z_0'], \qquad -[F_0''] = \frac{2}{\bar{R}^2} = [Z_0''] \tag{26}$$

and that, at any turning point, where $\mathrm{d}a/\mathrm{d}\bar{R} = 0$, the relation

$$\frac{2a + 1/\bar{R}}{a + a\coth(a\bar{R})} - \frac{2 + 1/\bar{R}}{1+\coth\bar{R}} = 0 \tag{27}$$

must be satisfied.

For any fixed heat of reaction $\tilde{Q}$, the implicit equation (25) can be solved numerically to provide the relationship between the heat-loss parameter a and the radius $\bar{R}$ of the reaction sheet within the flame ball. As can be seen in figure 2, there are no solutions for $\tilde{Q} \leqslant 1$. For

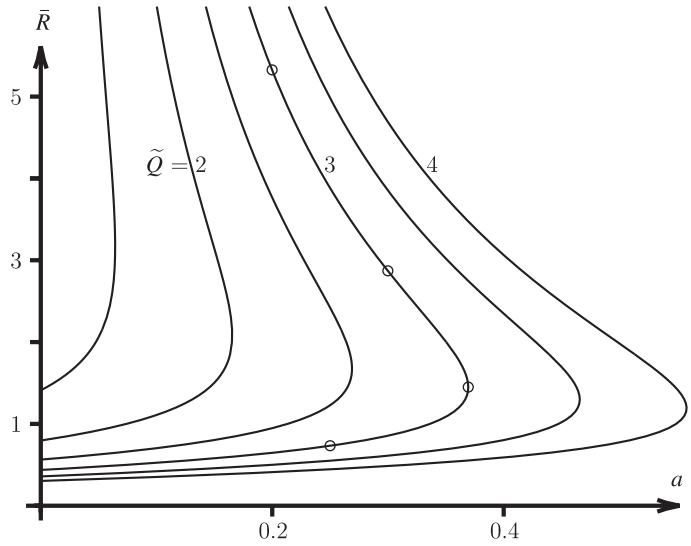

Figure 2. Relationship between the radius of the reaction sheet $\bar{R}$, at which fuel is consumed in a steady flame-ball solution, and the heat-loss parameter a, for constant values greater than unity of the scaled heat of reaction $\tilde{Q}$. Solution profiles at the points marked by the small circles are shown in figure 3.

larger values of $\tilde{Q}$, two branches of solution can be found. The lower branch, for any fixed $\tilde{Q}$, begins at an adiabatic solution ($a = 0$) with a finite value of $\bar{R}$. As a is increased, the radius $\bar{R}$ then increases gradually until a turning point is reached at a critical value $a = a_c(\tilde{Q})$, satisfying (27), with no solutions being possible at larger values of a. Above this turning point, there is a branch of solutions having a larger radius $\bar{R}$ that increases without bound as a is decreased towards zero. If $\tilde{Q}$ is increased, the turning point then occurs at larger values of a and, at any fixed value of a, $\bar{R}$ increases on the upper branch of solutions while it decreases on the lower branch.

The spatial variation of the fuel and radical concentrations and the temperature, at different points along one of the solution curves, is illustrated in figure 3. In these asymptotic solutions, the radical Z is produced at the spherical surface $r = \bar{R}$, where temperature has the value $T = 1$ and the fuel F is entirely consumed. Diffusion then spreads out the distribution of the radical which is also gradually consumed as it reacts to produce heat. The effect of heat loss is, of course, present in all of these solutions although it becomes more obvious at points that are further up the upper branch of solution; the top-left profile in figure 3, with the largest value of $\bar{R}$, has a local minimum of temperature at the centre of the flame ball. Another feature to note is that the maximum temperature is then not much above the critical temperature $T = 1$ at which the chain branching reaction is activated.

In fact, the maximum temperature is not very much greater than the critical temperature $T = 1$ in any of the solutions, even though a completely adiabatic flame ball, in which the scaled mass fractions of both F and Z might, hypothetically, be assumed to be zero at the origin, would have a maximum temperature of $T = \tilde{Q}$. For flame balls of large radius, the maximum temperature seems to be kept close to unity because of the effect of heat losses. For smaller flame balls, and those with a small heat-loss coefficient a, the temperature does not approach $\tilde{Q}$ because the radical concentration Z is not close to zero at the origin. Much of the chemical enthalpy is retained in the high radical concentration and is not released through being converted into the final products of the chemistry.

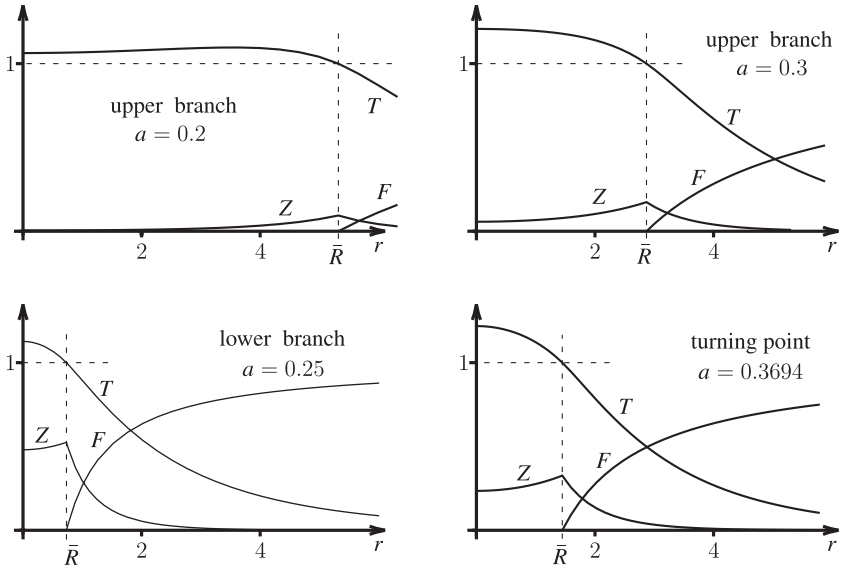

Figure 3. Profiles of steady solutions for temperature T and the normalized mass fractions F and Z of the fuel of the radical, respectively, at the points marked by the small circles in figure 2 on the solution curve for which the heat of reaction is $\tilde{Q} = 3$.

This restriction of the maximum temperature to the neighbourhood of a value that is generally well away from the fully reacted value of $T = \tilde{Q}$, is a feature that differs very significantly from flame balls modelled using one-step kinetics. In effect, the condition that $T = 1$ at the reaction sheet serves to anchor the maximum temperature around the value $T = 1$ on any branch of solution for any value of $\tilde{Q} > 1$; solutions automatically adjust themselves to meet the condition on temperature either through incomplete chemical conversion or through greater heat losses brought about by increasing the size of the flame ball. The numerical steady flame ball calculations of [43], carried out using a detailed chemical model for the oxidation of hydrogen, are entirely consistent with this observation; in [43] the maximum temperatures on all branches of solution over a wide range of equivalence ratios were only found to vary between about 900 and 1200 K. In this respect, the two-step model (2) produces results that are much closer to technically accurate models for flame balls than any one-step model.

For increasing values of $\bar{R}$, the tendency to limit the maximum temperature is made clearer in the profiles for T, F and Z that are shown in figure 4. As $\bar{R}$ is increased, the effect of heat loss is more and more strongly felt, leading to a significant reduction in the temperature inside the flame ball. At large values of $\bar{R}$, the temperature barely rises above $T = 1$ and the region in which the radical Z reacts to release heat occupies a relatively small portion of the overall spatial domain; the actual values of the radical concentration Z are also then seen to be relatively small.

As the equations (22) make clear, the radical concentration Z must decay over a range of values of r that is of order one around $r = \bar{R}$. The profiles in figure 4 are therefore reflecting the fact that this order one range is a relatively narrow part of the overall flame ball when $\bar{R}$ is large. Moreover, since the solution for F in (23) shows that $F_r = 1/\bar{R}$, at $r = \bar{R}^+$, which becomes small when $\bar{R}$ is large, the condition $[F_r]+[Z_r] = 0$ ensures that the values of Z must also be small, as seen in the solutions. At this stage, the solution closely resembles a solution that would arise if there was only a one-step chemical reaction F $\rightarrow$ P with F consumed and

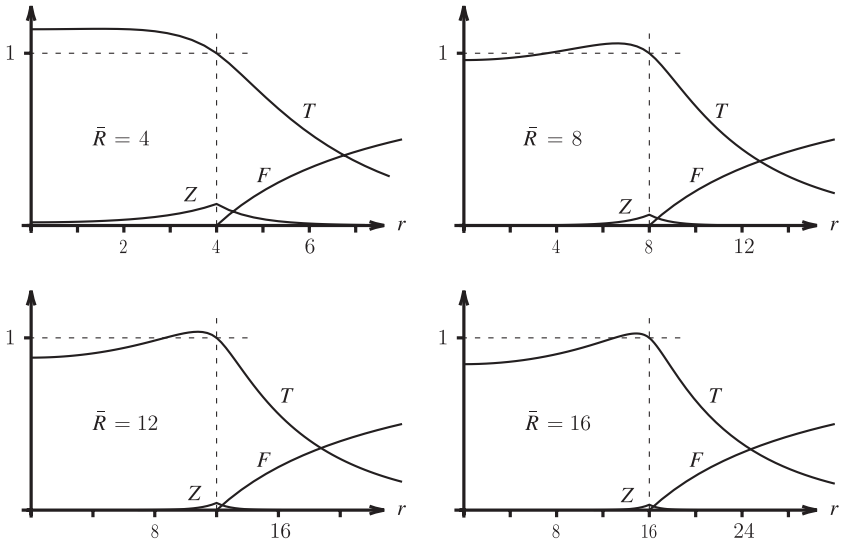

Figure 4. Profiles of steady solutions for temperature T and the normalized mass fractions F and Z of fuel and radical, respectively, for increasingly large steady radii $\bar{R}$ on the solution curve for which the heat of reaction is $\bar{Q} = 3$.

heat released entirely within a single narrow region where $T \approx 1$. This property has been explored further in [41] and is discussed in [42].

5.2. Comparison with numerical solutions

The solutions just described are leading order asymptotic solutions that are, strictly speaking, only accurate in the limit as $\beta \to \infty$. Whether the main features of the solutions are maintained for realistic values of β needs to be confirmed by solving the governing equations numerically.

Because the chain-branching kinetic model (2) is more realistic than the model (3) which involves fuel decomposition, only the dimensionless equations (6) were solved numerically, rather than the equations (14). However, one relatively minor change was introduced for numerical convenience; the dimensionless rate constant $k(T)$ was altered to the smooth and continuous function

$$k(T) = \max\left\{\left(e^{\beta(T-1)/3} - e^{1-\beta(2T+1)/3}\right)^3,\ 0\right\} \tag{28}$$

which produces exactly the same asymptotic limit, as $\beta \to \infty$, but which ensures that the chain branching reaction is completely eliminated in the cold gases at infinity. For all practical purposes, this definition of $k(T)$ behaves in very much the same way as does the definition in (6), for the same values of β, as illustrated in figure 5. The effect of changing q, which must lie between zero and one in value, is relatively minor wherever $k(T)$ is of order one. As a very robust means of testing the effect of finite Zeldovich number on flame balls, the formula (28) is therefore convenient.

In order to solve the equations (6) numerically on a finite grid, subject to the boundary conditions (7) at infinity, the transformation $r = \beta \tan(x/\beta)$ was used so that only a finite domain $0 \leqslant x \leqslant \frac{1}{2}\pi\beta$ needed to be discretized. Solutions were obtained using a standard finite difference approach, based on evenly spaced grid points in x, with continuation implemented using Newton iteration. A convenient way of calculating an effective steady radius $\bar{R}$, in the

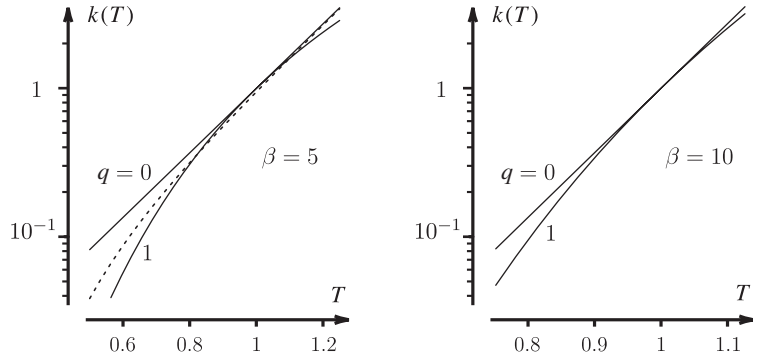

Figure 5. Different forms for $k(T)$: as defined using (6) with $q = 0$ or 1, shown by the solid curves; and as defined in (28), shown dotted. For $\beta \geqslant 10$ the formula (28) is graphically indistinguishable from (6) with $q = 0$. In all cases, with $\beta \geqslant 5$, it can be seen that $\ln k(T)$ is approximately linear in T, with slope β, near $T = 1$ where $k(T)$ is of order one.

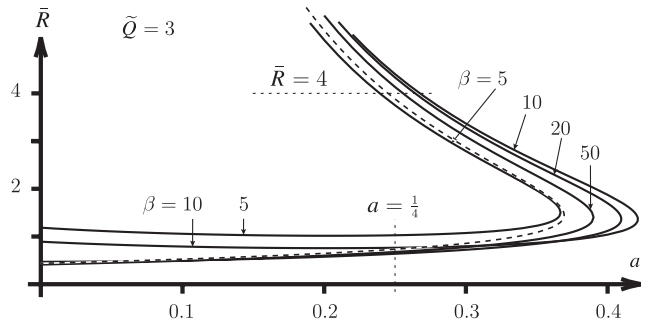

Figure 6. Comparison between the asymptotic solution, as $\beta \to \infty$ (- - - -), and numerical solutions (——) with $\beta = 5$, 10, 20 and 50, for steady flame balls involving simple chain-branching kinetics, in the case for which $\tilde{Q} = 3$. Profiles of temperature and the normalized mass fractions of fuel and radical, on the lower branch of solutions with $a = \frac{1}{4}$, are shown in figure 7, and on the upper branch with $\bar{R} \approx 4$, in figure 8.

spirit of [51], is to use the definition

$$\bar{R} = \frac{\int_0^\infty r^2 F Z k(T)\,\mathrm{d}r}{\int_0^\infty r F Z k(T)\,\mathrm{d}r}$$

which identifies the value of $\bar{R}$ that has the same effect outside the region of reaction, for a distributed reaction, as does a reaction that is concentrated on a thin sheet at $r = \bar{R}$.

Comparisons between the effective steady radii $\bar{R}$, calculated for some finite values of β, and the results as $\beta \to \infty$, are presented in figure 6, for a flame ball in which the heat of reaction is set to the representative value of $\tilde{Q} = 3$. It is interesting to note that, while the calculated values of $\bar{R}$ approach their asymptotic limit as β is increased, they do not do so monotonically. In fact, at $\beta = 5$ the values of $\bar{R}$ are closer to the asymptotic limit on the upper branch than they are for $\beta = 50$. More importantly perhaps, from the point of view of good modelling, the general qualitative character of the asymptotic solution is retained fully at entirely realistic values of the Zeldovich number β. This suggests that the asymptotic form of the model, as $\beta \to \infty$, can be used with relative confidence, even knowing that realistic values of β might not be much larger than about $\beta \approx 5$.

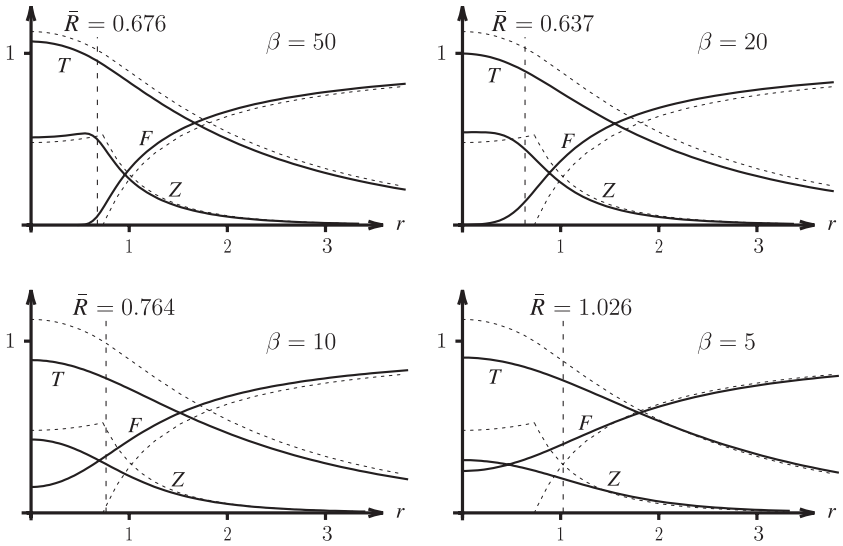

Figure 7. Profiles of steady solutions for temperature T and the normalized mass fractions of fuel F and radical Z, calculated with $\tilde{Q} = 3$ for different values of the Zeldovich number β on the lower branch of solutions where $a = \frac{1}{4}$. Dotted lines show the asymptotic solution as $\beta \to \infty$ and the dashed lines mark the effective radius $\bar{R}$ of a concentrated region of chain-branching reaction.

On the lower branch of solution, where the heat loss parameter has the value $a = \frac{1}{4}$, figure 7 demonstrates how the numerically calculated values of T, F and Z vary with r, for each of the values of β used in plotting figure 6. These can be compared with the dotted lines which show the asymptotic limit as $\beta \to \infty$ (also seen in the lower-left diagram in figure 3). The comparison is good at the larger values of β and it improves, as it should do, as β increases. At the lower values of β the thickness of the region of chain-branching reaction, which consumes the fuel F, increases, so that at $\beta = 10$ and 5, there are significant concentrations of fuel at the origin. Nevertheless it can be noted that, in moving away from the flame ball, the comparisons remain good in all cases at larger values of r. In spite of the chain-branching reaction becoming more distributed, its overall effect therefore remains very much the same.

In the case of the upper branch of solution, figure 8 presents numerically calculated variations of T, F and Z, for the same four values of β. In each case, the value of a was chosen so that $\bar{R} \approx 4$. These solutions can be compared with the dotted lines which present the asymptotic limit as $\beta \to \infty$ (also seen in the upper-left diagram in figure 4). Once again the comparison is good at the larger values of β, as it should be. At lower values of β the thickness of the region of chain-branching reaction can be seen to increase but because the effective radius $\bar{R}$ is larger on the upper branch, fuel concentrations now tend to remain low at the origin. In all cases, the comparisons remain good at larger values of r so that, once again, the overall effect of the chain-branching reaction is largely unaltered by changing the value of β.

These numerical results show that the overall nature of the solutions at relatively low values of β is captured very well by the asymptotic solutions found as $\beta \to \infty$. The comparison is better on the upper branch of solutions which, as we shall now demonstrate, is the branch on which stable flame balls can arise. Numerical studies of the linear stability of these flame-ball solutions were not carried out.

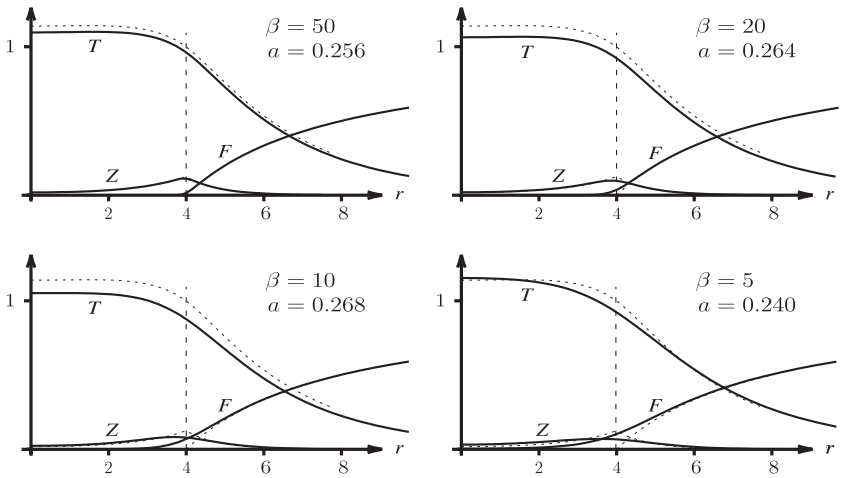

Figure 8. Profiles of steady solutions for temperature T and the normalized mass fractions of fuel F and radical Z, calculated with $\tilde{Q} = 3$ for different values of the Zeldovich number β, on the upper branch of solutions, with values of a chosen so that the effective radius of a concentrated region of chain-branching reaction, marked by the dashed lines, lies at $\bar{R} \approx 4$. Dotted lines give the asymptotic solution as $\beta \to \infty$.

5.3. Linear stability with spherical symmetry

If perturbations from the steady solutions are written in the form of normal modes with growth rate λ

$$R = \bar{R} + e^{\lambda t} \qquad F = F_0(r) + e^{\lambda t} F_1(r)$$
$$Z = Z_0(r) + e^{\lambda t} Z_1(r) \qquad T = T_0(r) + e^{\lambda t} T_1(r)$$

the linearized equations to be satisfied by the eigenfunctions F_1, Z_1 and T_1 are found to be

$$\begin{aligned} 0 &= T_1'' + 2r^{-1}T_1' - (\lambda + a^2)T_1 + \tilde{Q}Z_1 \\ 0 &= F_1'' + 2r^{-1}F_1' - \lambda \mathrm{Le_F} F_1 \\ 0 &= Z_1'' + 2r^{-1}Z_1' - (\lambda \mathrm{Le_Z} + 1)Z_1. \end{aligned} \tag{29}$$

For $r < \bar{R}$ there is no fuel at all, so that $F_1 \equiv 0$. Applying the jump conditions at $r = \bar{R} + e^{\lambda t}$, to Taylor expansions of T, F and Z about the point $r = \bar{R}$, shows that the conditions to be satisfied at $r = \bar{R}^{\pm}$ are

$$[F_0'' + F_1'] + [Z_0'' + Z_1'] = T_0' + T_1 = 0$$
$$[T_0'' + T_1'] = [T_0' + T_1] = [F_0' + F_1] = [Z_0' + Z_1] = F_0' + F_1 = 0.$$

Making use of equation (24), with $\bar{F} = 0$, and the relations (26) these conditions become

$$[F_1'] + [Z_1'] = [T_1'] = [T_1] = 0, \qquad F_1(\bar{R}^+) = [F_1] = -[Z_1] = -\frac{1}{\bar{R}}$$
$$T_1(\bar{R}) = \frac{\tilde{Q}}{\bar{R}^2(a^2 - 1)} \left(\frac{\bar{R} + 1}{1 + \coth \bar{R}} - \frac{\bar{R} + 1/a}{1 + \coth(a\bar{R})} \right).$$

The solution of equations (29) can be expressed most simply through defining

$$\mu^2 = a^2 + \lambda, \qquad \nu^2 = \lambda \mathrm{Le_F}, \qquad \delta^2 = 1 + \lambda \mathrm{Le_Z}. \tag{30}$$

Solutions satisfying $F_1(\bar{R}^+) = [F_1] = -[Z_1] = -1/\bar{R}$ and $[F_1'] + [Z_1'] = [T_1'] = [T_1] = 0$ can then be written as

$$F_1 = \frac{1}{r} \times \begin{cases} -e^{\nu(\bar{R}-r)} & \text{for } r > \bar{R} \\ 0 & \text{for } r < \bar{R} \end{cases}$$

$$Z_1 = \frac{1}{r} \times \begin{cases} \dfrac{\nu/\delta + \coth(\delta\bar{R})}{1+\coth(\delta\bar{R})} e^{\delta(\bar{R}-r)} & \text{for } r > \bar{R} \\ \dfrac{\nu/\delta - 1}{1+\coth(\delta\bar{R})} \dfrac{\sinh(\delta r)}{\sinh(\delta\bar{R})} & \text{for } r < \bar{R} \end{cases}$$

$$(\mu^2 - \delta^2)T_1 = \tilde{Q}Z_1 - \frac{\tilde{Q}}{r} \times \begin{cases} \dfrac{\nu/\mu + \coth(\mu\bar{R})}{1+\coth(\mu\bar{R})} e^{\mu(\bar{R}-r)} & \text{for } r > \bar{R} \\ \dfrac{\nu/\mu - 1}{1+\coth(\mu\bar{R})} \dfrac{\sinh(\mu r)}{\sinh(\mu\bar{R})} & \text{for } r < \bar{R}. \end{cases}$$

The remaining condition, fixing the value of T_1 at $r = \bar{R}$, finally provides the dispersion relation

$$\frac{1}{1-a^2}\left(\frac{\bar{R}+1/a}{1+\coth(a\bar{R})} - \frac{\bar{R}+1}{1+\coth\bar{R}}\right) = \frac{\bar{R}}{\delta^2-\mu^2}\left(\frac{\nu/\mu - 1}{1+\coth(\mu\bar{R})} - \frac{\nu/\delta - 1}{1+\coth(\delta\bar{R})}\right) \tag{31}$$

the solutions of which provide the spectrum of possible growth-rates. For stability, the real part of all roots λ must be negative.

In the case for which $\lambda = 0$ (a neutrally stable real eigenvalue) the dispersion relation reduces to the form

$$\frac{2a + 1/\bar{R}}{a + a\coth(a\bar{R})} - \frac{2 + 1/\bar{R}}{1+\coth\bar{R}} = 0$$

a result that is independent of the Lewis numbers and that corresponds exactly to the turning point or fold-bifurcation path (27) on which $\mathrm{d}a/\mathrm{d}\bar{R} = 0$. This makes it clear that one root is exactly zero at the turning point.

In order to understand the behaviour of other roots, at least qualitatively, it is useful to firstly consider only roots that are small in magnitude. Noting from (30) that ν involves the square root of λ, it is simplest to define $\lambda = \varpi^2$ and to consider the limit in which $|\varpi|$ is small. Expanding the dispersion relation (31) up to quadratic powers of ϖ then leads to

$$A\varpi^2 - B\varpi + C = \mathrm{O}(\varpi^3) \tag{32}$$

with the coefficients

$$\begin{aligned} C &= \frac{\tilde{Q}}{1-a^2}\left(\frac{2a+1/\bar{R}}{a+a\coth(a\bar{R})} - \frac{2+1/\bar{R}}{1+\coth\bar{R}}\right) \\ B &= \frac{\tilde{Q}\mathrm{Le}_\mathrm{F}^{1/2}}{1-a^2}\left(\frac{1}{a+a\coth(a\bar{R})} - \frac{1}{1+\coth\bar{R}}\right) = \mathrm{Le}_\mathrm{F}^{1/2}\bar{R} \\ 2A &= \frac{\mathrm{Le}_\mathrm{Z}-1}{1-a^2}(1+C) + \frac{\tilde{Q}\bar{R}}{1-a^2}\left(\frac{\mathrm{Le}_\mathrm{Z}(1-\coth\bar{R})}{1+\coth\bar{R}} - \frac{1-\coth(a\bar{R})}{a+a\coth(a\bar{R})}\right). \end{aligned} \tag{33}$$

It can immediately be noted from (27) that C is zero at the turning point. Closer inspection reveals that it is positive on the upper branch of solutions and negative on the lower branch. Figure 9 also shows that the values of C remain bounded between about -1 and 1 over the entire range of solutions for any fixed value of the heat of reaction $\tilde{Q}$. Both A and B are positive quantities, at least near the turning point, with B depending on the Lewis number of fuel Le_F

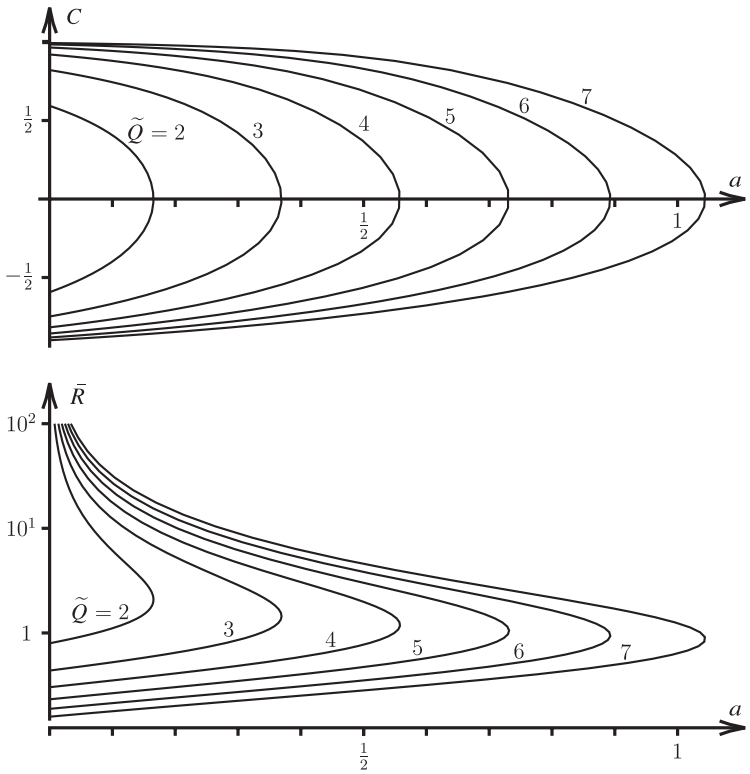

Figure 9. Upper figure: the relationship between the heat-loss coefficient a and the parameter C at a number of fixed values of the heat of reaction $\tilde{Q}$. Lower figure: corresponding solution paths in the space of a and $\bar{R}$ for the same fixed values of the heat of reaction. These figures demonstrate that C remains fairly small over a significant portion of each solution around its turning point.

(since it is simply given by $B = \mathrm{Le}_{\mathrm{F}}^{1/2}\bar{R}$) and with A depending, in a more complicated way, on the Lewis number of the radical Le_{Z}.

If A is written in the form

$$A = \tfrac{1}{2}A_0 + \tfrac{1}{2}A_1\mathrm{Le}_{\mathrm{Z}}$$

the coefficients A_0 and A_1, the expressions for which are contained in equations (33), are independent of the Lewis numbers and figure 10 shows that A_1 remains positive and order one over a wide range of values of $\tilde{Q}$ at the turning point $C = 0$. The value of A_0 grows without bound as $\tilde{Q}$ decreases towards unity while it decreases steadily as $\tilde{Q}$ increases. Both A_0 and A_1 are positive order one quantities at the turning point for order one values of $\tilde{Q}$ that are not close to unity. It can be seen from figure 11 that negative values of A_0 and A_1 can arise at non-zero values of C for large enough values of $\tilde{Q}$. In particular, A_0 becomes negative over a range of positive values of C when $\tilde{Q}$ is about five or larger and A_1 becomes negative over an increasingly large range of negative values of C as $\tilde{Q}$ increases above about two. For large enough values of $\tilde{Q}$ and/or Le_{Z}, the value of A can therefore become negative, although it is always positive near $C = 0$. While B is always positive, its value can be made arbitrarily small by decreasing the value of Le_{F}.

Truncated at quadratic orders, the dispersion relation (32) has the roots

$$\varpi \sim \frac{B \pm \sqrt{B^2 - 4AC}}{2A}.$$

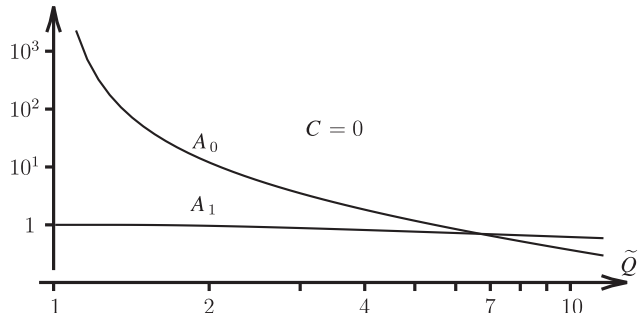

Figure 10. Dependence of the quantities A_0 and A_1 on the heat of reaction $\tilde{Q}$, evaluated at the turning point $C = 0$. The values of A_0, A_1 and C are instrumental in solving the dispersion relation (31) for small growth rates λ.

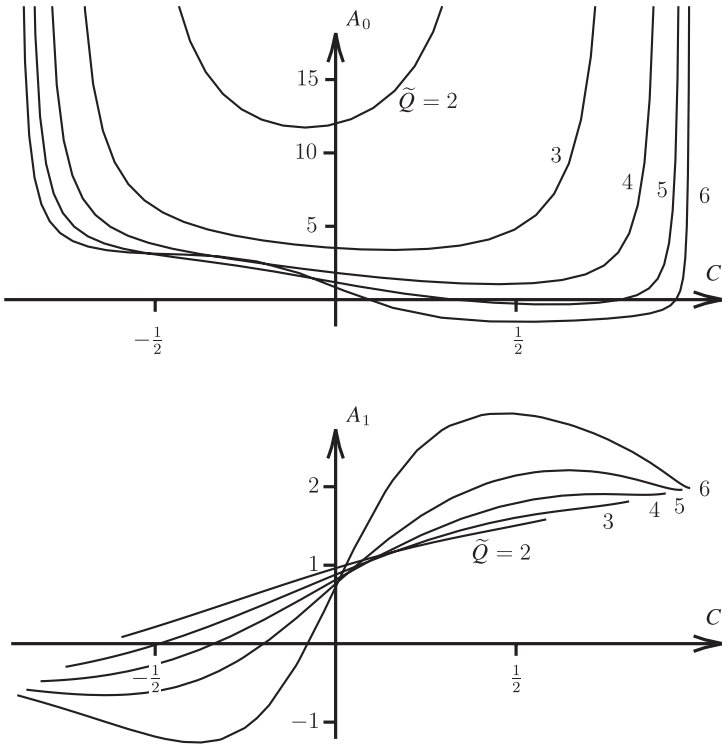

Figure 11. Variations of A_0 (upper diagram) and A_1 (lower diagram) with C at fixed values of the heat of reaction $\tilde{Q}$.

Stability requires that $\mathrm{Re}\,\lambda = \mathrm{Re}\,\varpi^2 < 0$ or, equivalently, that $|\mathrm{Im}\,\varpi| > |\mathrm{Re}\,\varpi|$. The criterion for stability, with $|\lambda|$ small, is therefore

$$2AC > B^2 \qquad \text{or} \qquad \mathrm{Le_F} < (A_0 + A_1 \mathrm{Le_Z}) \frac{C}{\bar{R}^2}. \tag{34}$$

This makes it clear that the flame ball is, in fact, unstable at the turning point, where $C = 0$; although one eigenvalue is zero there is another unstable real eigenvalue. Moreover, provided $A_0 + A_1 \mathrm{Le_Z}$ is positive, eigenvalues are found to be stable for small enough values of the Lewis

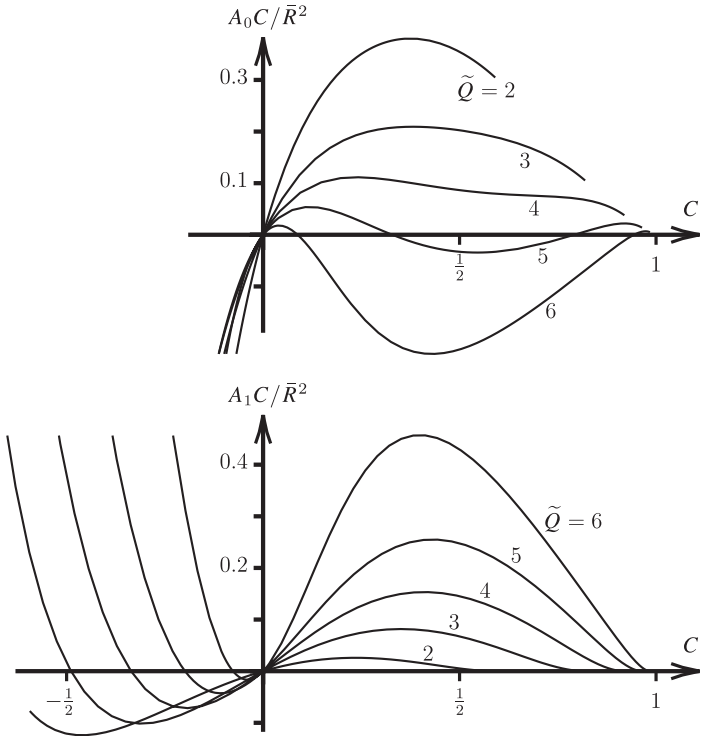

Figure 12. Variations of $A_0C/\bar{R}^2$ (upper diagram) and $A_1C/\bar{R}^2$ (lower diagram) with C at fixed values of the heat of reaction $\tilde{Q}$.

number $\mathrm{Le_F}$ on the upper branch where C is positive. Also, if $A_0 + A_1\mathrm{Le_Z}$ is negative and C is negative, then stability can again arise for small enough values of $\mathrm{Le_F}$.

A convenient way of examining the dependence of stability on $\mathrm{Le_F}$ and $\mathrm{Le_Z}$ is provided by examining the values of $A_0C/\bar{R}^2$ and $A_1C/\bar{R}^2$. According to (34) the value of $\mathrm{Le_F}$ must be less than the former plus $\mathrm{Le_Z}$ times the latter. As seen in figure 12, the largest values of $\mathrm{Le_F}$ for stability are determined by a combination of trends, with the contribution from A_0 decreasing and that from A_1 increasing as $\tilde{Q}$ increases. At any negative value of C, it can be seen that $A_0C/\bar{R}^2$ is very much more negative than $A_1C/\bar{R}^2$ is positive so that unrealistically large values of $\mathrm{Le_Z}$ would be required to bring about stability on the lower branch of solutions.

At the point where the flame ball becomes stable, λ has two purely imaginary roots, indicating that the instability has an oscillatory character near the point of marginal stability. The real roots found at $C = 0$ must therefore collide to form a complex conjugate pair, as C changes, before the real part of λ becomes negative.

This analysis, based on equations (32) and (33), depends on assuming that all eigenvalues λ are small. However it is, at least, consistent for them to be small if C is small, as it is near the turning point, once small enough values of $\mathrm{Le_F}$ are also chosen to ensure stability; under these conditions, the values of λ are of the order of C/A. It can also be noted from figure 9 that the values of C are reasonably small over a significant range of values of $\bar{R}$ around the turning point. The argument does therefore provide a consistent demonstration that stable flame balls can exist if $\mathrm{Le_F}$ is small enough. Particularly when A is large and positive, as it clearly is for order one values of $\mathrm{Le_Z}$, if $\tilde{Q}$ is not larger than about three, formula (34) offers a reasonable qualitative and quantitative explanation for the stability of the flame ball for small eigenvalues.

If the radical Lewis number $\mathrm{Le_Z}$ has a realistic order-one value, it then makes it clear that stability only arises on part of the upper branch for small enough fuel Lewis numbers $\mathrm{Le_F}$.

The possibility of having large unstable values of λ can be examined using the asymptotic relation

$$\left(2\varpi^3\mathrm{Le_Z} + (1 + a\mathrm{Le_Z})\varpi\right)\left(\frac{1}{\tilde{Q}} + \frac{C}{1-a^2}\right) + \frac{2\mathrm{Le_Z^{1/2}}}{1+\mathrm{Le_Z^{1/2}}} = O(\varpi^{-1})$$

which is valid, as $|\varpi| \to \infty$, provided ϖ has a large real part, taken to be positive without loss of generality, as it must be for instability. It is readily seen that the only large root is

$$\varpi \sim i\sqrt{\tfrac{1}{2}\left(a + \frac{1}{\mathrm{Le_Z}}\right)}$$

arising for $\mathrm{Le_Z} \ll 1$. However, being imaginary to leading order, this root represents stability. Thus there are no large unstable eigenvalues.

In order to complete the picture, for order one and for small eigenvalues, the full dispersion relation (31) can be studied numerically. This was done by searching for all eigenvalues with positive or order one real part over a wide range of conditions. The typical pattern that is found for stability is illustrated in figure 13 in the case for which $\mathrm{Le_Z} = 1$. For small enough values of $\mathrm{Le_F}$ a region of stability is found on the upper branch of the solution curves with a small enough heat of reaction $\tilde{Q}$. As the fuel Lewis number $\mathrm{Le_F}$ is decreased, the region of stability increases. And, as the heat of reaction is increased, the region of stability decreases. This picture is consistent with the findings of the more approximate analysis based on equations (32) and (33).

It is worth noting that stability analyses for one-step chemistry [29, 30, 38] also show that flame balls are stable to radially symmetric disturbances on their upper branch of solution, for

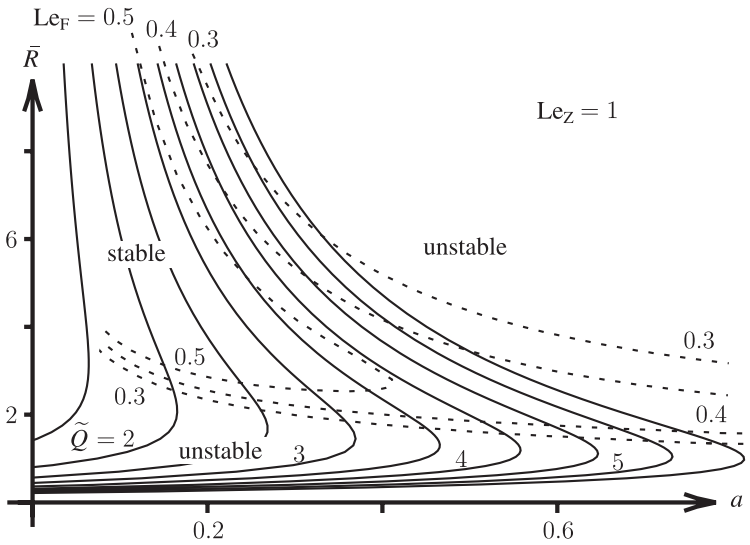

Figure 13. Stability of the flame-ball solutions. The solid curves are the paths at which steady radii $\bar{R}$ are found as a function of the heat-loss coefficient a. The dashed curves mark the boundaries for marginal stability at three different Lewis numbers of the fuel $\mathrm{Le_F}$, with the Lewis number of the radicals $\mathrm{Le_Z}$ set to unity. Between these curves, on the upper branches of solution, stable flame balls arise at low enough values of $\mathrm{Le_F}$.

fuel Lewis numbers that are below unity. However, there are also significant differences that arise for the model with chain-branching chemistry.

With one-step chemistry, part of the upper branch is always stable for any $\mathrm{Le_F} < 1$. Moreover, for radially symmetric disturbances, this stability extends to all radii larger than a threshold radius that approaches the turning point as $\mathrm{Le_F} \to 0$. However, for a given heat-release parameter $\tilde{Q} > 1$, stability only arises for the chain-branching model at fuel Lewis numbers that are below a threshold value that changes with $\tilde{Q}$ and $\mathrm{Le_Z}$. This range of stability initially only occupies a finite range of the upper branch of solutions and does not generally extend to all larger radii. As $\mathrm{Le_F}$ decreases further, the lower end of the range of stability approaches the turning point, as it does with one-step chemistry, and the upper end of the range of stability increases. Especially at lower values of $\tilde{Q}$, the numerical and approximate solutions of the dispersion relations (31) are not conclusive in establishing whether or not this range extends to all radii greater than the lower threshold for small enough values of $\mathrm{Le_F}$.

6. Conclusions

The use of a simple kinetic model, that involves only one thermally-sensitive autocatalytic chain-branching reaction that converts a fuel into radicals, which then release heat in a thermally-insensitive completion reaction, provides a self-consistent description of flame balls. Asymptotic solutions, based on allowing the activation temperature of the branching reaction to approach infinity, have the same overall qualitative character as solutions calculated numerically at finite and realistically low activation temperatures.

A slightly different model in which the fuel decomposes directly to produce the radical has exactly the same form of asymptotic solution as is found with the chain-branching reaction. Even though fuel decomposition reactions are actually negligible in hydrocarbon flames, this finding is significant. It indicates that the details of the processes that generate radicals are not as important as the simple fact that radicals are generated. Indeed, because numerical solutions preserve the same overall character when the Zeldovich number of the branching reaction is as low as five, the production of radicals only needs to occur in a moderately thermally-sensitive way in order to have qualitatively the same overall effect—even the quantative differences are found to remain relatively small.

Once produced, the role of the radicals is twofold. They act as a reservoir of chemical enthalpy so that the removal of fuel from the system is not translated directly into heat, as it is in any one-step chemical model. Also, because radicals are destroyed by the completion reaction to form products and heat, more slowly than they are created in the branching reaction, they have time to diffuse away from the relatively thin region within which they are created. As a result, heat is generated in a broader region within any flame. Another feature of the simple autocatalytic chain-branching model (2) for radical production, in which there is no decomposition mechanism for producing radicals, is that the reactant F remains stable at temperatures below the crossover temperature. There is therefore no cold boundary difficulty if the unburnt conditions are below this temperature.

The role of chemical radicals has not been exploited much in the study of flames from a mathematical and asymptotic perspective [6]. Using a one-step model for the chemistry, asymptotic studies have made great strides in examining many kinds of combustion phenomena. This article shows that relatively straightforward, and arguably more realistic, solutions can be obtained using the two-step models (2) and (3). At infinite Zeldovich numbers these provide a simple asymptotic reduction to a flame-sheet model at which the essentially linear jump conditions (18) apply. Resulting solutions are algebraically more complicated than their one-step counterparts, because radical concentrations have to be described in addition to fuel and

temperature, but they are nevertheless accessible to mathematical investigation in studying premixed flames.

In the case of flame balls, the overall bifurcation character and the appearance of stable structures on the branch of solutions with larger radius are broadly similar in nature to the analogous results found for one-step chemistry with infinite activation temperature [27–38], with some notable differences. It is found that stable flame balls arise, as an oscillatory form of instability becomes stable, if the Lewis number of the fuel species is made low enough. However stability first appears at Lewis numbers of the fuel that are below a threshold value which depends on the reactant concentration at infinity and the Lewis number of the radical, rather than simply being less than unity. Also, at least near the threshold Lewis number, the range of stability is finite on the branch of larger flame-ball solutions, increasing in size as the Lewis number of fuel is decreased.

The solutions themselves are also found to involve maximum temperatures that remain fairly close to the crossover temperature for hydrocarbon chemistry, rather than the adiabatic flame-ball temperature. Technically accurate numerical calculations of hydrogen-oxygen flame balls [43] also behave in this way, suggesting that the model with chain branching offers a closer representation of the real problem. This feature of the solutions arises through a combination of heat-loss effects and the fact that much of the chemical enthalpy can remain absorbed within a non-zero concentration of radicals, rather than being converted directly from fuel into heat, as the one-step model demands.

The model with chain branching can also be used to model planar premixed flames, as was first demonstrated by Zeldovich [14] for adiabatic flames with unit Lewis numbers. In more general situations, solutions are broadly analogous in their structure and dependence of propagation speed on heat loss, to solutions modelled using one-step chemistry [41], although there are some notable differences. There are still two propagation speeds for any small enough heat loss, with the slower speed always being unstable, but solutions based on the chain-branching model do not display the extreme sensitivity to maximum flame temperature that one-step models automatically involve at large activation temperature. Interestingly, another difference arises in that, while the leading order dimensional flame speed does depend on the Lewis number of radicals Le_{Z}, it is not found to depend on the Lewis number of the fuel Le_{F} [41].

Stability results for planar non-adiabatic premixed flames, based on the leading order model (17) and (18), have also now been calculated [52]. These are found to generate a cellular form of instability at fuel Lewis numbers that are sufficiently reduced below unity.

Acknowledgments

The authors are grateful to the EPSRC and the University of New South Wales for financial support.

References

[1] Williams F A 1965 *Combustion Theory* 2nd edn (New York: Addison-Wesley) (2nd edn 1985 (CA: Benjamin-Cummings))
[2] Zeldovich Ya B, Barrenblatt G I, Librovich V B and Makhviladze G M 1985 *The Mathematical Theory of Combustion and Explosions* (New York: Consultants Bureau)
[3] Buckmaster J D and Ludford G S S 1982 *Theory of Laminar Flames* (Cambridge: Cambridge University Press)
[4] Kapila A K 1983 *Asymptotic Treatment of Chemically Reacting Systems* (London: Pitman)
[5] Pelcé P 1988 *Dynamics of Curved Fronts* (London: Academic)
[6] Liñán A and Williams F A 1993 *Fundamental Aspects of Combustion* (New York: Oxford University Press)

[7] Peters N 2000 *Turbulent Combustion* (Cambridge: Cambridge University Press)
[8] Williams F A 1971 Theory of combustion in laminar flows *Ann. Rev. Fluid Mech.* **3** 171
[9] Sivashinsky G I 1983 Instabilities, pattern formation and turbulence in flames *Ann. Rev. Fluid Mech.* **15** 179–99
[10] Kassoy D R 1985 Mathematical modeling for planar, steady, subsonic combustion waves *Ann. Rev. Fluid Mech.* **17** 267–87
[11] Buckmaster J 1993 The structure and stability of laminar flames *Ann. Rev. Fluid Mech.* **25** 21–53
[12] Clavin P 1994 Premixed combustion and gasdynamics *Ann. Rev. Fluid Mech.* **26** 321–52
[13] Sivashinsky G I 2003 Some developments in premixed combustion modelling *Proc. Combust. Inst.* **29** 1737–62
[14] Zeldovich Ya B 1961 Chain reactions in hot flames—an approximate theory of flame velocities *Kinet. Kataliz* **11** 685 (as described in Zeldovich *et al* 1985 *op cit.* 397–401)
[15] Joulin G, Liñán A, Ludford G S S, Peters N and Schmidt-Lainé C 1985 Flames with chain-branching chain-breaking kinetics *SIAM J. Appl. Math.* **45** 420–34
[16] Mikolaitis D W 1986 Adiabatic flame speeds and the Zeldovich–Liñán model *Combust. Sci. Technol.* **49** 277–88
[17] Tam R Y 1988 Stretch response and large heat release in the Zeldovich–Liñán model *Combust. Sci. Technol.* **60** 125–42
[18] Tam R Y 1988 Damköhler number ratio asymptotics of the Zeldovich–Liñán model *Combust. Sci. Technol.* **62** 297–309
[19] Chao B H and Law C K 1994 Laminar flame propagation with volumetric heat-loss and chain branching-termination reactions *Int. J. Heat Mass Transfer* **37** 673–80
[20] Smooke M D (ed) 1991 *Reduced Kinetic Mechanisms and Asymptotic Approximations for Methane–Air Flames (Lecture Notes in Physics vol 384)* (Berlin: Springer)
[21] Peters N and Rogg B (ed) 1993 *Reduced Reaction Mechanisms for Applications in Combustion Systems (Lecture Notes in Physics, New Series vol m15)* (Berlin: Springer)
[22] Peters N 1997 Kinetic foundation of thermal flame theory *Prog. Astronaut. Aeronaut.* **173** 73–91
[23] Dold J W 1989 Flame propagation in a non-uniform mixture: analysis of a slowly-varying triple-flame *Combust. Flame* **76** 71–88
[24] Dold J W, Hartley L J and Green D 1991 Dynamics of laminar triple-flamelet structures in non-premixed turbulent combustion *IMA Math. Appl.* **35** 83–105
[25] Kioni P N, Rogg B, Bray K N C and Liñán A 1993 Flame spread in laminar mixing layers—the triple flame *Combust. Flame* **95** 276
[26] Vederajan T G, Buckmaster J and Ronney P 1998 Two-dimensional failure waves and ignition fronts in premixed combustion *Proc. Combust. Inst.* **27** 537–44
[27] Joulin G 1985 Point source initiation of lean spherical flames of light reactants: an asymptotic study *Combust. Sci. Technol.* **43** 99–113
[28] Buckmaster J D and Joulin G 1989 Radial propagation of premixed flames and $\sqrt{t}$ behaviour *Combust. Flame* **78** 275–86
[29] Buckmaster J D, Joulin G and Ronney P 1990 The structure and stability of nonadiabatic flame balls *Combust. Flame* **79** 381–92
[30] Buckmaster J D, Joulin G and Ronney P 1991 The structure and stability of nonadiabatic flame balls: the effects of far-field losses *Combust. Flame* **84** 411–22
[31] Ronney P D, Whaling K N, Abbudmadrid A, Gatto J L and Pisowicz V L 1994 Stationary premixed flames in spherical and cylindrical geometries *AIAA J.* **32** 569–77
[32] Ronney P D, Wu M S, Pearlman H G and Weiland K J 1998 Experimental study of flame balls in space: preliminary results from STS-83 *AIAA J.* **36** 1361–8
[33] Ronney P D 1998 Premixed laminar and turbulent flames at microgravity *Space Forum* **4** 49–98
[34] Buckmaster J and Joulin G 1991 Flame balls stabilized by suspension in fluid with a steady linear ambient velocity distribution *J. Fluid Mech.* **227** 407–27
[35] Buckmaster J D and Joulin G 1993 Influence of boundary-induced losses on the structure and dynamics of flame-balls *Combust. Sci. Technol.* **89** 57–69
[36] Joulin G, Kurdyumov V N and Liñán A 1999 Existence conditions and drift velocities of adiabatic flame-balls in weak gravity fields *Combust. Theory Modelling* **3** 281–96
[37] Gerlinger W, Schneider K and Bockhorn H 2000 Numerical simulation of three-dimensional instabilities of spherical flame structures *Proc. Combust. Inst.* **28** 793–9
[38] Shah A A, Thatcher R W and Dold J W 2000 Stability of a spherical flame ball in a porous medium *Combust. Theory Modelling* **4** 511–34
[39] Minaev S, Kagan L, Joulin G and Sivashinsky G I 2001 On self drifting flame balls *Combust. Theory Modelling* **5** 609–22
[40] Joulin G, Cambray P and Jaouen N 2002 On the response of a flame ball to oscillating velocity gradients *Combust. Theory Modelling* **6** 53–78

[41] Dold J W, Thatcher R W, Omon-Arancibia A and Redman J 2003 From one-step to chain-branching premixed-flame asymptotics *Proc. Combust. Inst.* **29** 1519–26
[42] Dold J W, Thatcher R W and Shah A A 2003 High order effects in one-step reaction-sheet jump conditions for premixed flames *Combust. Theory Modelling* **7** 109–27
[43] Buckmaster J, Smooke M and Giovangigli V 1993 Analytical and numerical modeling of flame-balls in hydrogen–air mixtures *Combust. Flame* **94** 113–24
[44] Abid M, Wu M S, Liu J B, Ronney P D, Ueki M, Maruta K, Kobayashi H, Niioka T and Vanzand D M 1999 Experimental and numerical study of flame ball IR and UV emissions *Combust. Flame* **116** 348–59
[45] Wu M S, Ronney P D, Colantonio R O and Vanzandt D M 1999 Detailed numerical simulation of flame ball structure and dynamics *Combust. Flame* **116** 387–97
[46] Tse S D, He L and Law C K 2000 A computational study of the transition from localized ignition to flame ball in lean hydrogen/air mixtures *Proc. Combust. Inst.* **28** 1917–24
[47] Glassman I 1987 *Combustion* (2nd edn) (London: Academic) (3rd edn 1996)
[48] Westbrook C K 2000 Chemical kinetics of hydrocarbon ignition in practical combustion systems *Proc. Combust. Inst.* **28** 1563–77
[49] Flynn P F, Hunter G L, Farrell L, Durrett R P, Akinyemi O, Zur Loye A O, Westbrook C K and Pitz W J 2000 The inevitability of engine-out NO_x emissions from spark-ignited and diesel engines *Proc. Combust. Inst.* **28** 1211–8
[50] Dibble R W, Warnatz J and Maas U 2001 *Combustion: Physical and Chemical Fundamentals, Modeling and Simulation, Experiments, Pollutant Formation* (Berlin: Springer)
[51] Law C K, Chao B H and Umemura A 1992 On closure in activation energy asymptotics of premixed flames *Combust. Sci. Technol.* **88** 59–88
[52] Dold J W 2003 Premixed flames with thermally sensitive intermediate kinetics (submitted)